U.S. Department of Homeland Security
Science and Technology Directorate
International Programs Division

Rail Vehicle Fire Hazard Guidance

Grant #2009-ST-108-000013

Final Summary Report
June 2, 2010

ARUP

U.S. Department of Homeland Security
Science and Technology Directorate – International Programs Division

Rail Vehicle Fire Hazard Guidance

Grant #2009-ST-108-000013

Final Summary Report

June 2010

Brian J. Meacham, PhD, PE
Nicholas A. Dembsey, PhD, PE
Kurt Schebel

ARUP

Jeffrey S. Tubbs, PE
Matthew A. Johann, PE
Amanda Kimball, PE
Andrew Neviackas

Worcester Polytechnic Institute
Department of Fire Protection Engineering
100 Institute Road, Worcester, MA 01609
Tel +1 508 831 5593 Fax +1 508 831 5862
www.wpi.edu

Arup USA, Inc
955 Massachusetts Avenue, 4th floor, Cambridge, MA 02139
Tel +1 617 864 2987 Fax +1 617 864 6178
www.arup.com

This report takes into account the particular instructions and requirements of our client.
It is not intended for and should not be relied upon by any third party and no responsibility is undertaken to any third party

Job number 209884

Contents

Tables

Figures

Appendices

Acknowledgement

This material is based upon work supported by the Science & Technology Directorate, U.S. Department of Homeland Security, under Award Number 2009-ST-108-000013.

Disclaimer

The views and conclusions contained in this document are those of the authors and should not be interpreted as necessarily representing the official policies, either expressed or implied, of the U.S. Department of Homeland Security.

Executive Summary

Whether a small fire in a passenger rail vehicle stays small or grows to encompass the vehicle, and how large the ultimate fire may become, is largely a function of the initiation fire, vehicle interior materials (interior lining / components and contents), vehicle configuration and ventilation. Assuming fixed configuration and limited ventilation options, significant variables become the initiation fire, interior materials and contents.

Evaluation of the relative fire hazards represented by different interior lining materials as exposed to various initiation fire scenarios can be costly and time-consuming if full-scale fire tests are utilized. However, small-scale fire tests, such as those that utilize the cone calorimeter apparatus, are less expensive (by far) and numerous tests can be carried out in a given day. Small-scale test data, coupled with initiation fire data and computational modeling, can be used to cost-effectively assess a wide range of scenarios and material combinations for existing and proposed vehicle designs.

Although computational modeling has been used for some time, previous generation tools lacked the sophistication to address several important features, including flame spread and contribution of interior lining materials.

This report has proposed a methodology for determine flame spread and fire growth behaviors within rail vehicles based upon small-scale fire tests. Through the application of a relatively-simple screening tool capable of identifying a material's propensity to spread flames, a spreadsheet-based initial flame spread prediction methodology, and computational fluid dynamics fire modeling tools, prediction of the overall fire hazard represented by a given vehicle configuration is possible.

The proposed methodology has been demonstrated through a hypothetical scenario in which two possible lining materials were compared. The approach demonstrated that one of these materials was not appropriate given the stated stakeholder goals, while a second material represented an acceptable level of fire hazard. This analysis was not intended to represent a specific vehicle or rail system, but rather was used to demonstrate how the proposed methodology could be applied.

The methodology outlined in this report has several potential applications, including the following:

Fire hazard assessment of existing stock: Whereas it is costly to burn complete vehicles to understand fire development issues, this approach allows for small samples of materials to be tested (from an existing vehicle, or from parts for a vehicle), and analysis to be conducted to obtain an indication as to what size initiation fire might lead to full vehicle involvement, and what the resultant fire size would be. This could be used as part of a threat, vulnerability and risk assessment (TVRA) of vehicles to understand impacts on passengers and other vehicles.

Fire hazard assessment of critical infrastructure: As noted above, this methodology can be applied to help better understand the resultant fire size from a fully-involved vehicle. This could be used as part of a threat, vulnerability and risk assessment (TVRA) stations, tunnels and other rail infrastructure to assess impact from the vehicle fire. This could range from smoke control in a station to thermal impact on tunnel lining or bridge decking. This could be applied to existing infrastructure or to new designs. With a current focus on high-speed rail, for example, such an approach may be beneficial for assessing a wide range of potential fire scenarios – accidental or deliberate – and to support assessment of mitigation options.

Options analysis for new vehicle design: At the vehicle design stage, the methodology can be applied to help assess the performance of different interior lining materials with respect to resistance to initiation fires of concern and contribution to overall fire size. Manufacturers can use this information to make informed judgments about material use in vehicles. With a current focus on high-speed rail, for example, such an approach may be beneficial for assessing a wide range of vehicle options.

Regulatory support: Current regulations generally require testing of material flame spread at a single heat flux level (e.g., see the 2008 report prepared for the FTA [6]). As demonstrated by this research; however, a material may perform differently at different heat flux levels, such as resisting ignition and self-propagating flame spread to lower levels, to igniting and self-propagating flame at higher heat flux levels. Based on the level of risk or hazard deemed tolerable from a regulatory perspective, this methodology could be used as support for modifying flame spread test requirements, such as perhaps requiring a range of incident heat fluxes and reporting outcomes. With a current focus on high-speed rail, for example, it may be anticipated that new materials will be suggested, and new or more robust testing may be desired to understand how material perform as part of regulatory benchmarking.

More extensive computational modeling, over a broader range of materials, vehicle configurations, and ventilation conditions would be helpful in identifying and addressing uncertainty in the computational modeling and from refining the efficacy of the methodology for the potential applications outlined above.

Tools for threat, vulnerability and risk assessment (TVRA) and regulatory analysis and policy setting could be developed based on the methodology. Options might range from providing a more formalized structure for the basic concepts outlined herein, to development of more risk-informed performance-based analysis techniques for fire hazard analysis, to development of risk-cost optimization approaches or models for setting regulatory targets.

1 Introduction

This report is intended to summarize the work carried out by Worcester Polytechnic Institute and Arup regarding the development of a methodology to support evaluation of fire development and spread hazards associated with passenger rail vehicle interior lining materials.

1.1 General Description

In general, fire in a passenger rail vehicle will be influenced by the type, amount and characteristics of available fuel (e.g., interior lining and seating materials and contents), ventilation and compartment (vehicle) configuration. For any given combination of these parameters, the size and location of an initiating fire within a train car can significantly affect the ultimate fire size. Factors such as the effects of adjacent materials on fire spread and growth, interaction of the fire with the geometric elements of the car, and the potential for flame spread away from the fire origin must be considered. For instance, a fire initiating on the floor adjacent to a stainless steel panel and away from any seats will not likely grow to a significant size because of the absence of fuel. However, a fire on a seat directly adjacent to a clear plastic advertisement panel that extends upwards to a plastic laminate ceiling panel may result in significant flame spread and a large ultimate fire size. Better understanding of the relationship between initiation fire and interior lining materials, and the influence of these on the maximum fire size that may be expected, is critical to fire hazard analysis for existing and new vehicles. Using this information to estimate how large a fire in a passenger rail vehicle might grow will help better inform risk and hazard assessments of critical rail infrastructure, including stations and tunnels, as well as vehicles themselves.

1.2 Goals

The goals of this research study are to advance our ability to estimate the maximum potential fire sizes for common train configurations and materials used within rail cars in the United States given a range of initiation fire scenarios. The fundamental goals of this analysis are to:

- Understand the range of vehicles configurations that are commonly used, with a focus on subway and commuter rail vehicles.
- Understand the range of interior materials that are commonly used, with a focus on combustible interior lining.
- Understand what size initiation fires can lead to self-propagating fires given the combustible interior materials which are used.
- Determine if a flashed-over (fully developed) fire can be expected to occur within common rail car configurations.
- Determine the expected total heat release rate (power output) per rail car.

1.3 Scope

The scope of this research study will be limited to interior portions of passenger rail cars as can be expected to be used within the United States. Specifically, rail car configurations for both subway and standard commuter/passenger trains will be analyzed. Locomotive cars are not within the scope of this research. This study will attempt to define common rail car configurations and their fundamental interior material properties. These inputs will then be used as inputs into fire models to analyze the expected fire hazard based on varying initiation size fires.

The exterior portions of trains will be assumed to not contribute to the fire hazard potential of trains as preliminary research has indicated only noncombustible materials are used for the exterior shell.

The scope of this research study will be as follows:

- Determine common configurations and sizes for passenger rail cars used within the United States.
- Determine common material properties used in rail cars within the United States. Determine the material thermo-physical properties based upon cone calorimeter test data.
- Develop a methodology to evaluate the relative fire hazards associated with different lining materials.
- Demonstrate the application of the proposed methodology.

It has been assumed that the scope of this research will not include the following factors:

- Tunnel draft effects and effects of air flow through the train in the event that the end doors are open for passenger egress during a fire within the train
- Train motion (either a train with a fire or other trains in the tunnel system)
- Occupant intervention (suppression efforts)
- Materials other than those described in the referenced train design documents and in this report
- Fires located on the exterior of (under, adjacent to, or distant from) a train
- Occupant egress from a train
- Post-collision structural failure
- Locomotive rail cars

1.4 Key Issues

1.4.1 Train Configurations

Within the United States a large number of rail cars exist. Depending upon the location or the type of train (subway, commuter rail, high speed train etc.), a vast number of rail cars all with different sizes and material compositions can be found. Understanding, evaluating and grouping these various rail cars into common groups is a key issue that is imperative to this study. Research has already indicated that train sizes vary considerably throughout the United States.

1.4.2 Material Properties

The fire protection research community has developed significant amounts of data regarding the combustion characteristics of various fuels. However, given the vast number of materials used in products, vehicles, and buildings, data is often not available to fit a specific design. This is true of the majority of the materials used in the Toronto Rocket Trains. While data may be available regarding similar materials, such data may be misleading and can decrease the accuracy of the analyses because it does not take into account the actual combustion characteristics of the specific materials being used.

1.4.3 Flame Spread Modeling

Modeling flame spread is challenging due to its strong dependence on material thermal properties, model geometry, and computational mesh size. It is envisioned that CFD modeling will be the primary means of estimating the fire potential of various rail cars. It should be noted, that while CFD is capable of modeling flame spread, it should be used for order-of-magnitude estimates only given the uncertainty inherent in the calculations. This approach will require significant knowledge of the computational methodologies of the CFD model and the material property inputs specific to the CFD model.

Because flame spread modeling is a new science and involves cutting-edge technology, there will be numerous uncertainties associated with this type of work. Full-scale fire tests will not be included within the scope of this work, and as such calibration of flame spread models against partial-scale mockup fire tests will be a vital part of this research study. Material properties will be estimated by simulating cone calorimeter tests using the sub-model in FDS and to find the set of material properties that provides optimal agreement between experimental data and model prediction.

1.5 Acronyms

Acronyms used within this report are defined as follows:

ASTM	American Society for Testing and Materials
CFD	Computational fluid dynamics
CHF	Critical heat flux
FDS	Fire Dynamics Simulator
FRP	Fiber-reinforced plastic
GA	Genetic algorithm
GRP	Glass-reinforced plastic
HRR	Heat release rate
HRRPUA	Heat release rate per unit area
LES	Large eddy simulation
NASFM	National Association of State Fire Marshals
NFPA	National Fire Protection Association
NIST	National Institute of Standards and Technology
SFPE	Society of Fire Protection Engineers

2 Literature Review

2.1 NFPA 130

NFPA 130, *Standard for Fixed Guideway and Passenger Rail Systems,* provides minimum safety requirements including "life safety from fire and fire protection requirements for underground, surface, and elevated fixed guideway transit and passenger rail systems, including but not limited to stations, trainways, emergency ventilation systems, **vehicles**, emergency procedures, communications, control systems, and vehicle storage areas" [1].

Vehicle requirements within NFPA 130 focus on the location of high voltage electrical equipment, fuel tanks and the flammability and smoke emission characteristics of materials. Specifically, NFPA 130 requires materials to be tested for surface flammability to not exhibit any flaming running or dripping. In addition, testing of a complete seat assembly including its cushions, fabric layers etc., is required to be performed in accordance with ASTM E1537 and meet the pass/fail criteria of the California Technical Bulletin 133. NFPA 130 also states that a fire hazard analysis is required to occur which considers the environment where the seat is located. Specifically, such aspects as cuts or punctures within the seat cushion that could be caused by vandalism and additional combustibles that could increase the fire hazard are all required to be considered within the analysis.

In addition, NFPA 130 states that any carpeting within vehicles is required to be tested in accordance with ASTM E162 and ASTM E662. All other components such as HVAC ducting, acoustical insulation, light diffusers, windows, gaskets, wire and cable, structural components etc., are all required to be tested in accordance with certain ASTM standards and demonstrate performance criteria such as flame spread ratings below defined thresholds. NFPA 130 continues to define further fire safety requirements by providing very strict electrical requirements to wires, motors and other equipment.

If these aforementioned prescriptive requirements cannot entirely be met, NFPA 130 allows an engineering analysis, known as a performance based analysis, to occur as well. This allows vehicles to be designed to meet the objectives and criteria established within the engineering analysis and the general fire safety requirements within NFPA 130. These general goals are to fundamentally provide occupant protection, structural integrity of the vehicle and maintain system effectiveness.

2.2 Fire Hazard Evaluation of the Interior of WMATA Metrorail Cars

NBSIR 75-971, *A Fire Hazard Evaluation of the Interior of WMATA Metrorail Cars*, authored by Emil Braun describes the test results of a series of fire tests conducted for the Washington Metropolitan Area Transit Authority, which were conducted to assess the potential fire hazard of the Metrorail cars. Small-scale laboratory tests were conducted on material samples, full-scale fire tests were completed on mock-ups of the interior, and a smoke penetration test was carried out on a real car.

The seat cushions tested as part of the full-scale tests included an integral skin urethane foam seat, a vinyl-covered neoprene foam seat, as well as a blank seat (no combustible cushion) to measure the contribution of the wall material on the fire. The evaluation criteria used for the full-scale tests were that there be no significant spread of fire from the seat of ignition and that the smoke level shall be such to allow egress in a reasonable time from a burning car. Data recorded for the full-scale tests included temperature, smoke intensity, and concentrations of CO, CO_2, and O_2.

The small-scale tests completed per FAR 25.853, which is a Federal Aviation Administration test for small-scale fire performance for compartment interior materials on transport

category airplanes, demonstrated satisfactory fire performance. However, the full-scale experiments demonstrated that was not true in their end-use configuration. Although, the fire did not spread to another seat when the cushion was made of vinyl-covered neoprene foam (when located on the aisle and not next to a wall), the tests involving the urethane seating had fire spread from one seat to another. In addition, the wall material added to the fire spread between seats. Hazardous levels of smoke that would reduce vision were developed in five minutes for the urethane seats and nine minutes for the neoprene seats.

The smoke penetration test on the floor demonstrated that the floor assembly should be effective in preventing the passage of smoke into the car from an undercarriage fire and would provide ten minutes of protection.

2.3 Fire Hazard Evaluation of BART Vehicles

NBSIR 78-1421, *Fire Hazard Evaluation of BART Vehicles*, written by Emil Braun documents a fire hazard evaluation that was completed for subway cars used for the San Francisco Bay Area Rapid Transit (BART). The fire hazard analysis was completed by identifying fire scenarios based on the design of the subway cars and associated systems as well as the materials used in the car and seating. Recommendations included upgrading the flame resistance of the seat assemblies by using vinyl upholstery, investigating feasibility of using intumescent coating on the wall and ceiling liner, developing a means for hardening the floor assembly against undercarriage fire penetration, and installing a fire detection system in the subway cars.

2.4 Fire Safety Guidelines for Vehicles in a Downtown People Mover System

NBSIR 78-1586, *Fire Safety Guidelines for Vehicles in a Downtown People Mover System*, written by Richard Peacock describes a fire safety aspects study of people movers located in urban areas. This study included a review of existing and planned vehicles so internal and external fire scenarios could be developed. From this study, the report presents guidance for design of downtown people mover systems and recommendations for fire and smoke detection and fire suppression equipment.

Recommendations for the interior of the vehicle included that the space below seats be enclosed to prevent potential ignition below the seats, using non-combustible materials, not using upholstery on the seats, and using carpeting over plymetal for the flooring. In addition, it was suggested that two different emergency exits be provided – one at each end of the car – as well as smoke detector in the main a/c system return air ducts and hand-held fire extinguishers provided in each car.

The report also provides guidelines for testing of materials to be used in people mover cars.

2.5 Fire Tests of Amtrak Passenger Rail Vehicle Interiors

Fire Tests of Amtrak Passenger Rail Vehicle Interiors written by R.D. Peacock and E. Braun describes a series of tests completed for Amtrak vehicles, which included both full-scale mock-up tests, calorimeter tests, and small-scale material tests. The full-scale mock-ups consisted of floor, wall, and ceiling panels and two double seat assemblies. Measurements were made for temperature, heat flux, velocities, gas concentration, smoke density, and rate of heat release. The calorimeter tests were completed with just a full-scale seat cushion and seat back.

Results of the small-scale tests on the individual materials were found to predict the trends in the full-scale fire performance. However, when geometry was changed, the small-scale

test could not predict the effect of the change. Specific recommendations resulting for the testing included looking into alternatives for the carpeted luggage rack, eliminating padded armrests, and ensuring the material used as a wall covering will resist ignition.

2.6 Fire Safety of Passenger Trains

NIST Technical Note 1406, *Fire Safety of Passenger Trains: A Review of Current Approaches and of New Concepts*, by Richard Peacock, Richard Bukowski, Walter Jones, Paul Reneke, Vytenis Babrauskas, and James Brown details a study completed comparing fire safety approaches used internationally as well as current methods for measuring fire performance.

Specifically, the fire safety approaches of the United States, France, and Germany were reviewed. Then, the authors present a system approach to fire safety based on the approaches of these three countries as well as other material. The paper also explores scenario based modeling of fire hazards. From this review and analysis several recommendations are made for updates to the U.S. guidelines.

2.7 Fire Safety of Passenger Trains – Phase I: Material Evaluation

NISTIR 6132, *Fire Safety of Passenger Trains: Phase I: Material Evaluation (Cone Calorimeter)*, written by Richard Peacock and Emil Braun presents the results of the first phase of a three phase study. The objective the study was to demonstrate the practicality and effectiveness of heat release rate based test methods (i.e. Cone Calorimeter) and fire hazard analysis methodology in quantifying the threat of catastrophic fire conditions in a passenger train environment. The first phase was the evaluation of passenger train interior materials using the Cone Calorimeter test method, which were compared with data from small-scale test methods.

Various materials were tested using the Cone Calorimeter test method to get heat release rate data. This data will be used as part of the future phases of the project. For the majority of materials, the Cone Calorimeter results provided a good correlation with the small-scale test results.

2.8 Fire Safety of Passenger Trains; Phase II: Fire Hazard Analysis Techniques

NISTIR 6525, *Fire Safety of Passenger Trains; Phase II: Application of Fire Hazard Analysis Techniques*, authored by Richard Peacock, Paul Reneke, Jason Averill, Richard Bukowski, and John Klote presents the results of the second phase of a three phase study. The objective the study was to demonstrate the practicality and effectiveness of heat release rate based test methods (i.e. Cone Calorimeter) and fire hazard analysis methodology in quantifying the threat of catastrophic fire conditions in a passenger train environment.

This phase focused on hazard analysis techniques using heat release data and computer modeling to evaluate passenger rail car fire performance. The test data gathered during the first phase (see above) was used as an input to a computer fire model and analyses were completed on three different passenger car configurations.

2.9 Fire Safety of Passenger Trains; Phase III: Full-Scale Passenger Rail Car Tests

NISTIR 6563, *Fire Safety of Passenger Trains; Phase III: Evaluation of Fire Hazard Analysis Using Full-Scale Passenger Rail Car Tests*, authored by Richard Peacock, Jason Averill, Daniel Madrzykowski, David Stroup, Paul Reneke, and Richard Bukowski presents the

results of the third phase of a three phase study. The objective the study was to demonstrate the practicality and effectiveness of heat release rate based test methods (i.e. Cone Calorimeter) and fire hazard analysis methodology in quantifying the threat of catastrophic fire conditions in a passenger train environment.

This paper reports the results from a real-scale evaluation of the fire hazard analysis techniques used in the second phase (see above) of the study. The paper also presents comparisons of the real-scale test results with small- and full-scale results conducted in previous phases. The comparison of time to untenable conditions measured from these experiments and from the computer modeling completed during phase two showed agreement within 13%.

3 Passenger Rail Vehicle Characteristics

3.1 General Rail Vehicle Configurations

Research has indicated that the types, sizes, and material composition of rail-cars used within the United States vary significantly. Passenger rail cars, however, come in the following fundamental forms, listed with some examples below:

3.1.1 Subway

Subway vehicles come in numerous forms. The primary difference between these is the orientation of the passenger compartment and seating / standing provisions. Figure 1 through Figure 3 show some typical subway configurations.

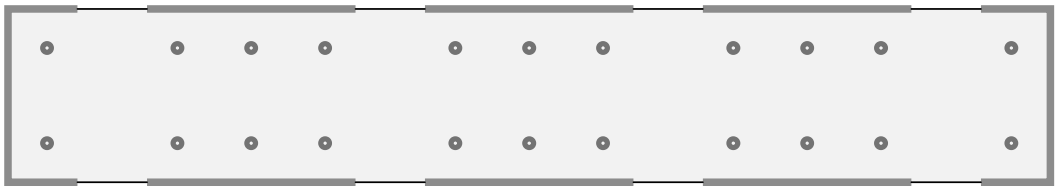

Figure 1. Subway Vehicle – Standing Only

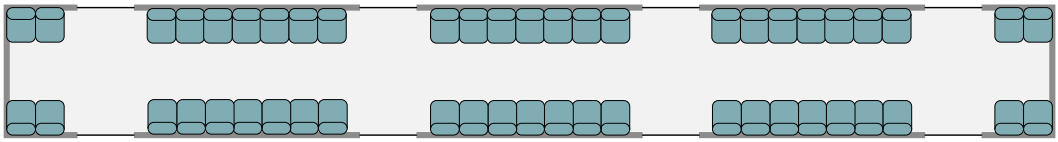

Figure 2. Subway Vehicle – Parallel Seating Only

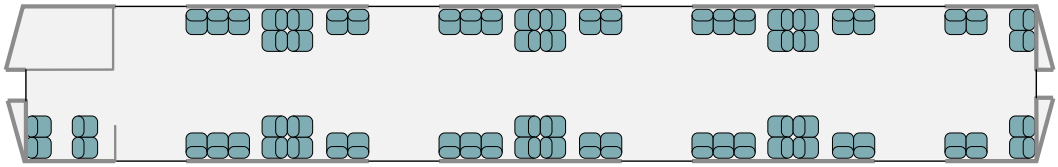

Figure 3. Subway Vehicle – Parallel and Perpendicular Seating

3.1.1.1 Examples of Subway Vehicles

Examples of subway vehicles include the following:

- Boston – “T”
- Chicago – “L”
- Miami – “Metrorail”
- New York City Subway
- Washington DC – “Metro”

Figure 4. Chicago Blue Line [2].

Figure 5. Exterior view of the NYC R62 train [3].

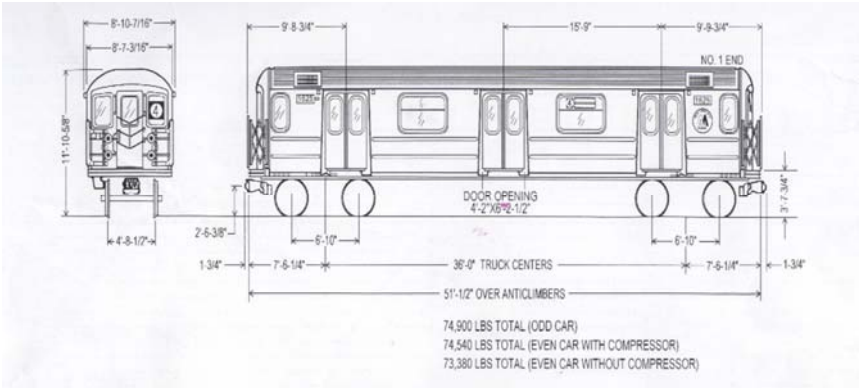

Figure 6. Dimensions of the NYC R62 train [3].

3.1.2 Commuter Rail Vehicles

Commuter rail vehicles generally include seating for most or all passengers. While some systems include vehicle designs similar to Figure 2 or Figure 3, most use perpendicular seating as shown in Figure 7.

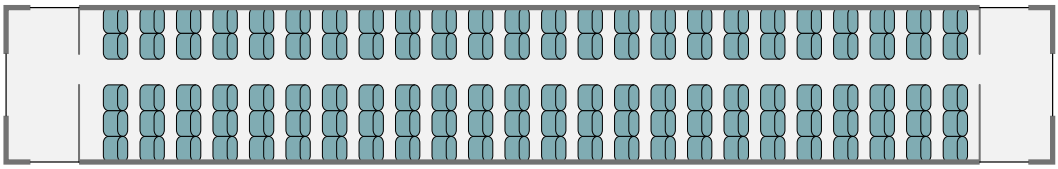

Figure 7. Commuter Rail Vehicle – Perpendicular Seating

3.1.3 Examples of Commuter Rail Vehicles

Examples of commuter rail vehicles include the following:

- Massachusetts – "MBTA"
- Long Island – "LIRR"
- New York – "Metro-North Railroad"
- New Jersey – "NJT"

Figure 8. Exterior view of the Massachusetts commuter rail [4].

3.1.4 High-Speed Passenger Rail Vehicles

High-speed rail vehicles are typically used over long distances and thus generally include comfortable seating for all passengers. They also often include additional amenities, such as restrooms and food-service areas. A typical high-speed rail passenger vehicle is shown in Figure 9.

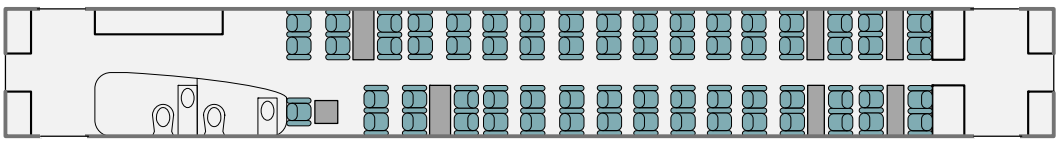

Figure 9. High-Speed Rail Passenger Vehicle

3.1.5 Examples of High-Speed Passenger Rail Vehicles

While numerous high-speed rail projects are planned for the US, the primary example currently in use is Amtrak's Acela. High-speed rail systems are much more common in Europe and Asia.

3.2 Rail Vehicle Dimensions

Table 1 illustrates the various general sizes of rail cars throughout the United States.

Table 1. Typical sizes of rail cars throughout the United States.

City/State/Region	Type of Rail Car	Line	Model	Manufacturer	Approximate Interior Car Width (ft)	Approximate Interior Car Length (ft)	Approximate Interior Car Height (ft)
New York [3]	Subway	A	R62	Kawasaki Heavy Industries	7.6	48.04	8.0
New York [3]	Subway	B	R32	Budd Co.	9	57.25	8.07
New York [3]	Subway	B	R42	St. Louis Car Co.	9	57	8.07
New York [3]	Subway	B	R68	Westinghouse Amrail Co.	9	72	8.07
New York [5]	Subway	B	142A	Kawasaki Heavy Industries	50	5.59	8.0
New York [3]	Subway	B	R143	Kawasaki Heavy Industries	8.77	57.21	8.12
Chicago [2]	Subway	Blueline	2200	Budd Co.	8.33	45	8.2
Washington DC	Subway		1000	Breda	9	72	8
Massachusetts [4]	Commuter Rail	MBTA	BiLevel Coach	Kawasaki Heavy Industries	9	82	13.75
Maryland [4]	Commuter Rail	MTA	BiLevel Coach	Kawasaki Heavy Industries	9	82	13.79
Long Island [4]	Commuter Rail	LIRR	BiLevel Coach	Kawasaki Heavy Industries	8.87	82	12.71
United States	Commuter Rail	Amfleet	Amfleet I/II	Budd Co.	9.5	82	10.91

3.3 Interior Material Properties

Depending upon the type and purpose of a rail vehicle and the requirements of the operators and users, a variety of materials may be present. These represent a wide range of combustibility characteristics that must be considered when evaluating fire hazards.

3.3.1 Common Passenger Rail Vehicle Materials

The following table lists example materials that are commonly used in passenger rail vehicles in the US. While individual users may require unique materials, this list is considered to be representative.

Table 2. Typical Materials in Passenger Rail Vehicles

Element	Typical Materials
Floors	• High pressure laminate • Carpet • Rubber-based sheet flooring
Walls	• Fiber-reinforced plastic panels • Plastic (melamine, fiber-reinforced plastic, etc.) • High pressure laminate • Metal (often aluminum or stainless steel)
Ceilings	• Plastic (melamine, fiber-reinforced plastic, high pressure laminates, etc.) • Metal (often aluminum or stainless steel)
Moldings / trim	• Metal (often aluminum or stainless steel) • Plastic (melamine, fiber-reinforced plastic, high pressure laminates, etc.)
Seats	• Fabric • Fiber-reinforced plastic • Carpet-like material
Doors	• Metal (often aluminum or stainless steel) • Plastic (melamine, fiber-reinforced plastic, high pressure laminates, etc.) • Glass windows
Windows	• Glass • “Lexan” plastic
Displays and signage covers	• Glass • “Lexan” plastic
Other	• Rubber • Nylon • Wood • Steel

3.3.2 Properties Required for Evaluation

In order to evaluate the contribution of different materials to the overall fire hazard represented by a given vehicle, certain material properties must be known. These properties serve as inputs to fire models that in turn can be used to evaluate fire growth and spread.

Key material property inputs required for fire growth and flame spread analysis using computational fluid dynamics methodologies may include the following:

- Molecular weight
- Density
- Chemical composition
- Material thickness
- Emissivity
- Soot yield
- Heat of combustion
- Heat of vaporization
- Thermal conductivity
- Specific heat

4 Review of Initiating Fire Scenarios

This section presents a review of historical rail fires compiled by Arup and by the National Association of State Fire Marshals (NASFM) for the Federal Transit Administration (FTA) [6] to result in a representative sampling of fires that have impacted passenger rail systems around the world, with a focus on location of the initial fire (e.g., within vehicle, under carriage, in tunnel or station, etc), probable ignition source, probable first materials burning, and outcome.

4.1 Review of Past Rail Fire Incidents

The purpose of collecting this data is to inform the range of initiation fire scenarios, including common ignition sources, initial material, initial fire sizes, and vehicle materials involved. A summary matrix including these parameters is included in Appendix A. The principal component of this research task involves searches using Lexis-Nexis to identify, obtain and review published articles where passenger rail vehicles were involved in fire events. The matrix, shown in Appendix A, documents a series of scenarios, which range from February of 2000 to November of 2009.

Review of this database suggests that the majority of the fires originated outside of the train: underneath the train, on the tracks, from exhaust, etc. Likewise, the report developed for the FTA indicates that 27% of U.S. rail transit fires between 1999 and 2002 were caused by mechanical failure or malfunction [6]. Although these 'external' fires generally have a limited direct impact on passenger life safety, they still result in significant operational problems as well as life safety issues related to exposure to smoke during egress. Injuries associated with fires originating outside of passenger compartments are generally related to smoke inhalation.

In general, a large portion of fires, both exterior and interior, appear to be caused by electrical issues such as surges and short circuits. Other failures, including leaks/breaks, cutting/welding close to combustible materials, or the mechanical failure of engine cars can also lead to fires. The severity of these events can depend on a number of variables, including the first materials ignited, adjacent materials, train configurations, occupant parameters, and location (e.g., within station, tunnel, etc).

Intentional ignition events have resulted in some of the most significant losses. The Daegu subway fire of February 18, 2003 in South Korea demonstrates shows how multiple contributing factors can lead to significant events. This event alone killed 198 people and injured at least 147. The arsonist was reported to be an older, deranged man with a known medical history, who set light to two milk cartons filled with flammable liquids. This fire spread quickly, and six cars were fully engulfed within two minutes [7]. The New York Times also reported that these trains were not equipped with fire extinguishers, subway personal were poorly trained for such events, sprinkler and ventilation systems failed since they were not linked to back up power, and the emergency signals were considered faulty. Investigators further reported that these cars were built with highly flammable materials that led to such rapid flame development and deemed the main reason as to why so many lives were lost in this event. Some of these highly flammable materials include vinyl, polyester and various other plastic materials [7].

Since intentional ignition within passenger vehicles is an essential variable to consider, additional focus is given to this type of reported event. From the information assessed, scenarios involving intentional ignition often include larger amounts of fuel (e.g., stacked seating materials or papers stacked on seats) and in some cases involved flammable liquids. Flammable liquids reported as being used in such events include gasoline, paint

thinner, propane in canisters, and other flammable substances often brought onto the train via milk jugs or spray cans and hidden in large duffel bags or cases.

4.2 Assessment of Initiation Fires

A range of initiating fire scenarios is possible in a passenger rail vehicle. Different scenarios will involve different initially-ignited fuels, and the ultimate fire size associated with these fuels is an important factor in determining if the initiating fire will lead to involvement of interior lining materials. Figure 10 depicts typical flame heights and heat flux levels resulting from a range of burning items. Heat flux levels are measured approximately 0.3 m (1.0 ft) from the fire. An office workstation is included for comparison.

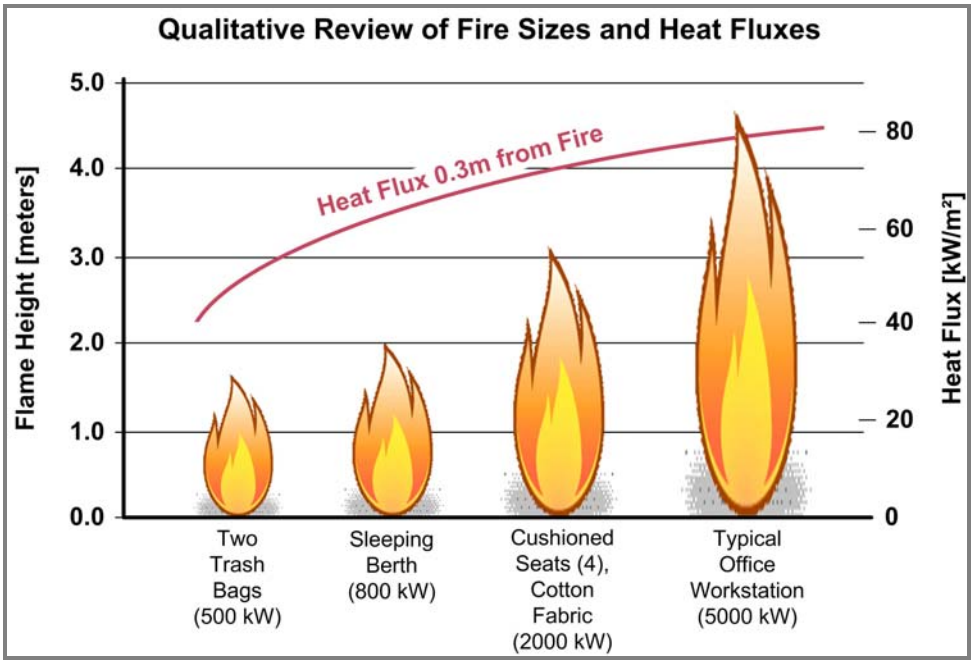

Figure 10. Relative Fire Sizes and Heat Fluxes

Once one has an understanding of the size of initiation fires, it is important to then be able to characterize them in such a way as to assess the likelihood of fire spread. In general, the issues of concern are intensity (temperature and radiant heat flux) and duration of fire in relation to the material which may next become ignited (for example, a match can easily ignite a thin piece of paper, but will not be able to ignite a thick block of wood).

In order to quantify whether an initiating fire is likely to spread to adjacent lining materials, the thermal exposure resulting from the initial fire needs to be reviewed. The following discussion considers an example material – fiber-reinforced plastic (FRP) with a gelcoat surface – to demonstrate how an initiating fire can be evaluated.

To evaluate whether or not a material will ignite under a given fire exposure, one must evaluate the material's critical heat flux (CHF). CHF is defined as the minimum heat flux at or below which a material does not generate vapors to support combustion. The parameters used to calculate CHF are external heat flux and time to ignition, both derived using the cone calorimeter. Figure 11 illustrates the external heat flux versus time to ignition for FRP Gelcoat. Theoretically, the time to ignition decreases exponentially as the external heat flux increases. At an external heat flux of 20 kW/m^2, it is shown that the time to ignition is likely to reach an infinite value, resulting in a CHF of 20 kW/m^2.

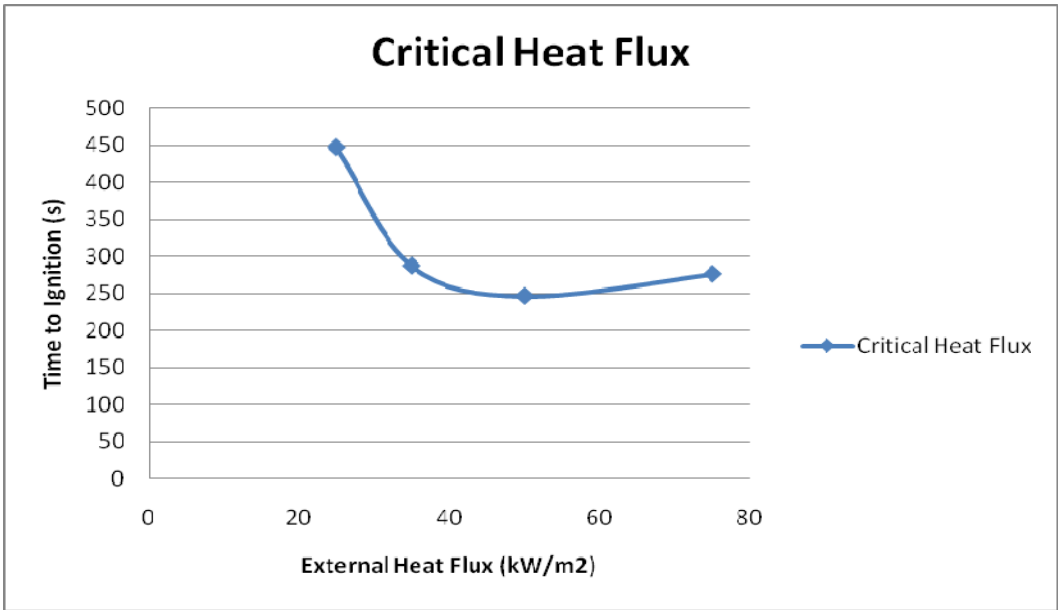

Figure 11. Critical Heat Flux

With this, it is necessary to compare thermal exposures calculated from cone calorimeter data to thermal exposures for the scenario at hand. This method can be used as a comparison tool to help quantify if the fire scenario is likely to ignite initial materials with conditions similar to that of the cone calorimeter.

The thermal exposure within the cone calorimeter can be calculated using the following formula.

$$(\dot{q}'' - CHF) * t_{ig} \qquad \text{[Eq. 1]}$$

Thermal exposures for FRP Gelcoat at multiple external heat fluxes can be seen in Table 3.

Table 3. Cone Calorimeter Thermal Exposure

External Heat flux (kW/m^2)	Ignition Time (s)	Thermal Exposure (kJ/m^2)
25	447	2,235
50	246	7,380

Heat flux exposures to lining materials will depend on the item burning and its proximity to the lining materials. Scenarios of interest in a passenger rail vehicle setting include trash bags, suitcases, vehicle seats [8], and flammable liquids, as discussed previously.

Based on work by Heskestad, a 50 percentile intermittent flame height can be developed using the following equation. It is important to keep in mind that the intermediate flame height is time varying because the HRR varies with time.

$$Z_f = 0.23\dot{Q}^{2/5} - 1.02D \qquad \text{[Eq. 2]}$$

Where,

Z_f = The 50 percentile intermittent flame height (m)

$\dot{Q}$ = The heat release rate (kW)

D = The diameter of the fire (m)

It is assumed that the radiative fraction (X_R) is 0.35. This is a reasonable approximation for the materials being reviewed.

The surface area of the flame can be calculated using Equation 3. Because intermediate flame height is time varying, the calculated surface area of the flame is also time varying.

$$A_{fl} = Z_{fl} * \pi D \qquad \text{[Eq. 3]}$$

For this discussion, the view factor ($F_{t\text{-}fl}$) is assumed to be one. This represents a case in which the fire is in very close proximity to the adjacent material. If the initial burning material is separated from the wall by some distance, the heat flux will be reduced; this would require calculation of the view factor.

Once values are obtained for the aforementioned parameters, it is important to define the thermal exposure in the context of the critical heat flux for each scenario. This is done with the following equation:

$$\int_0^t F_{t-fl}\left(\frac{\chi_R \dot{Q}}{A_{fl}}\right) - CHF \qquad \text{[Eq. 4]}$$

To calculate the exposure for each scenario, the heat flux histories above the critical values need to be integrated. This is accomplished accounting for the various time steps and the sum of the positive trapezoidal areas. The thermal exposures for a variety of scenarios are shown in Table 4.

Table 4. Thermal Exposures from Various Fire Scenarios

Scenario	Thermal Exposure (kJ/m^2)
Trash bags	4,029
Hard suitcase	5,625
Soft suitcase	N/A
Sleeping berth	9,835
Double seat	8,173

Using thermal exposure as a comparative tool, one can see that every scenario, except that of the soft suitcase, will result in a thermal exposure greater than that indicated by the cone calorimeter data collected at a heat flux of 25 kW/m^2.

In the case of the soft suitcase, thermal exposure values in excess of the CHF were not observed, so ignition of the example FRP material is not expected.

The sleeping berth and the double seat fires result in thermal exposure levels that are similar to that experienced in the cone calorimeter with a heat flux of 50 kW/m².

Further discussion on initiating fires is included in Section 7.4.5.6.

5 Fire Hazard Analysis Methodologies

As discussed in Section 2 of this report, numerous studies have been performed in regards to analyzing the fire hazard of interior materials in trains through full scale or partial scale fire tests. While conducting these full scale fire tests provides a true sense to the inherent fire hazard these materials present; running these experiments is not always feasible or cost effective. Performing computer models to analyze and predict the fire hazard within trains can provide a cost effective alternative to performing full scale fire tests.

Computer modeling has greatly improved over the last decade through computational fluid dynamics (CFD) programs such as Fire Dynamics Simulator (FDS) as developed by NIST. These modeling tools when combined with powerful optimization algorithms to estimate material properties can be utilized to estimate flame spread behavior within trains.

5.1 Introduction

Modeling flame spread between different materials and objects, and the resulting growth in fire hazard, is challenging due to its strong dependence on material thermal properties, model geometry, and computational mesh size. Modern computational fluid dynamics (CFD) models are capable of modeling flame spread; however, in most cases, they must be used for order-of-magnitude estimates only given the uncertainty inherent in this calculation. This approach requires significant knowledge of the computational methodologies of the CFD model and the material property inputs specific to the CFD model.

Because flame spread modeling is a relatively new science and involves cutting-edge technology, there are numerous uncertainties associated with this type of work. Calibration of flame spread models against full- or partial-scale mockup fire tests can provide greater confidence in the results.

5.2 Material Property Determination

Computational analysis methodologies require a range of input parameters, and the quality of the results is directly dependant on the quality and accuracy of these inputs. The modeling of fire growth and flame spread relies heavily on accurate descriptions of material properties. Determining values for these properties is accomplished through a mix of reviewing existing peer-reviewed research, carrying out small- or intermediate-scale fire tests, and extrapolating required quantities from known parameters.

5.2.1 The Cone Calorimeter

The cone calorimeter is one of the most widely used bench-scale fire testing apparatus for evaluating a material's flammability. It is an ASTM [9] and ISO [10] standardized apparatus that uses oxygen consumption calorimetry [11] to measure the heat release rate of a small-scale material specimens. Additional information can be found in *The SFPE Handbook of Fire Protection Engineering*, including a review of the cone calorimeter [12] and the general topic of fire calorimetry [13]. A typical cone calorimeter is shown in Figure 12.

Figure 12. Typical Cone Calorimeter

Cone calorimeter tests involve exposing a specimen measuring 0.1 m by 0.1 m (~0.01 m^2) to a constant external radiant flux by passing an electrical current through the cone-shaped heating element. The radiant flux incident to the sample surface can be varied between 0 and 100 kW/m² by changing the power output to the cone heater. Fire performance and burning characteristics can thus be evaluated under different heat flux conditions. Both theory and experiment indicate that the heat release rate increases as the radiative heat flux to a sample's surface increases. Thus, cone calorimeter testing at several flux levels is usually required to properly evaluate a material's flammability characteristics.

5.2.2 Data Extraction

Several material properties required for fire growth modeling using computational fluid dynamics modeling techniques cannot be directly measured with the cone calorimeter; however, they can be derived from the cone test data. The basic approach taken here is to simulate the cone calorimeter tests using the CFD program's sub-model that handles solid heating and gasification (usually called a "pyrolysis model") and to find the set of material properties that provides optimal agreement between the experimental data and model prediction. The FDS pyrolysis model [14] is a mathematical representation of the complex physical and chemical processes that occur in a solid when it is heated at fire-level heat fluxes. These processes include heat transfer, thermal decomposition (also called degradation or gasification), and mass transfer from the solid to the adjacent oxidizer.

Specialized laboratory tests such as thermo-gravimetric analysis and differential scanning calorimetry can be used to estimate some (but not all) of the material properties needed for fire modeling. However, these tests are expensive, especially if the assembly being modeled consists of several distinct materials as in the case of most modern trains. Furthermore, since these tests typically use very small samples with a mass of a few milligrams, they may not adequately represent real-world gasification or bulk combustion. Even if detailed property values were obtained from specialized tests, additional bench-scale testing (e.g. cone calorimeter) would still be required to determine each material's effective heat of combustion, species yields, and total heat content. Thus, it is more efficient and cost effective to estimate the material properties required for computer fire modeling from cone calorimeter testing.

Unfortunately, there is a disconnect between existing techniques for determining fire properties from cone calorimeter test data and the actual material properties needed to

model fire growth with CFD models such as FDS. Thermal ignition theories [15] can be used to determine a material's apparent thermal inertia (the product $k\rho c$) and its effective ignition temperature T_{ig}. However, the pyrolysis model in FDS requires individual thermal properties (k, ρ, c), and conventional data reduction techniques give only the product $k\rho c$. Furthermore, the $k\rho c$ and T_{ig} derived from existing data reduction techniques are apparent or effective values that depend on the environmental conditions [16]. While useful for establishing relative rankings and correlating ignition data [17], effective values are not useful for numerical fire modeling (e.g. FDS). Finally, there are no procedures available for readily determining the char thermal properties (k_c, ρ_c, c_c) or Arrhenius rate coefficients typically used to quantify the temperature-dependency of gasification rates.

Several methods are available to estimate the material properties needed for pyrolysis modeling from cone calorimeter or similar other bench-scale fire tests. The methodology proposed for use here involves the application of a genetic algorithm (GA) approach [18][19].

A GA is a type of stochastic optimization tool that is inspired by the concept of Darwinian evolution or natural selection, sometimes called survival of the fittest. Essentially, a random number generator is used to guess hundreds of different combinations of model input parameters (in this case material properties). The GA then uses the actual pyrolysis model to simulate a small scale fire test using the set of material properties it has guessed. The GA's calculations are compared to the results of the fire tests and the "fitness" of each parameter set is determined by quantifying how well the pyrolysis model calculations match the experimental data. These fitness values are then used to rank each parameter set from highest (best fitness) to lowest (worst fitness). The GA then uses these fitness values to determine which members of the parameter set are more promising. Through iteration, this process can eventually converge on a solution that can be considered optimal.

Typically, tens of thousands of trial solutions are required for convergence. The technique is heuristic; that is a good or near optimal solution can be found, but there is no guarantee that the best or optimal solution is found.

Figure 13 demonstrates the concept of the genetic algorithm working in unison with the FDS computer model. A material burned in the cone calorimeter provides the actual predicted mass loss rate as illustrated in the "thick green" curve. Several genetic algorithm computations are performed where the FDS pyrolysis model is used to sift through thousands of potential material property values. Through the use of a fitness function, or a measure of the trial solutions mass loss rate as predicted by FDS compared to the cone calorimeter data leads to a set of best fit material properties. The curves illustrated below represent the genetic algorithm's best estimation of material properties that produce similar heat release rate curves. The curves from the FDS simulation (as given inputs by the genetic algorithm) do not exactly match the curve of the cone test measurements because the underlying physical model is a simplification of the actual chemical and physical processes, which is a limitation of FDS. The peak rate of mass loss (directly proportional to heat release rate) is under predicted, yet the tail of the curve is over predicted. This example, however, illustrates that the computer model tends to show the same general shape as the curve derived from the cone test.

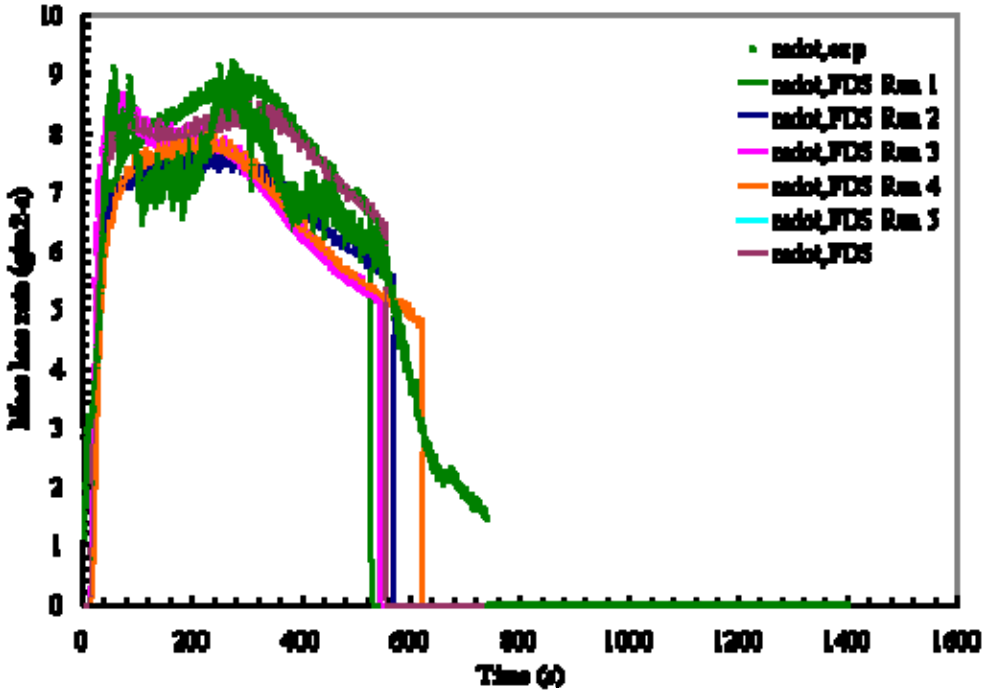

Figure 13. Example Comparison of Mass Loss Rates – Cone Calorimeter vs. FDS

6 Methodology for Vehicle Fire Hazard Assessment

6.1 Overview of Methodology

The proposed methodology for evaluating the fire hazard of passenger rail vehicle interior materials is summarized in Figure 14.

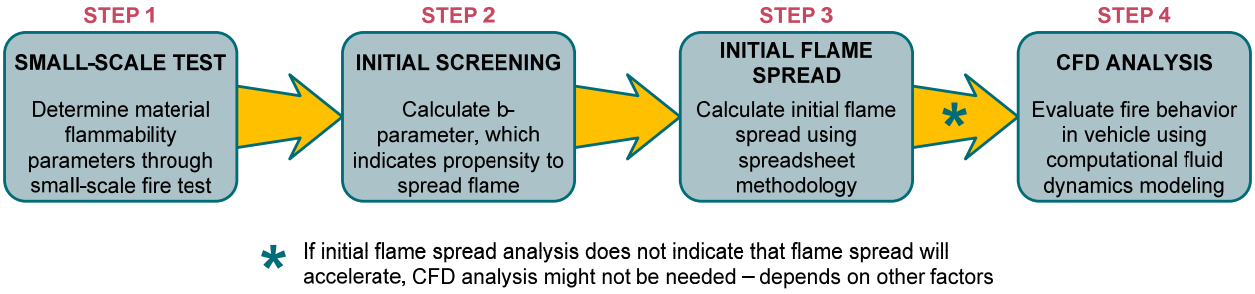

Figure 14. Overview of Vehicle Fire Hazard Assessment Methodology

There may be instances when the above process can be concluded after the second or third step. If the initial screening tool determines that the materials in question all have a minimal propensity to spread flame, then the engineer might conclude that the associated fire hazard is also minimal. The fire protection engineer should consider numerous other factors, including possible initiating fires, ventilation conditions, etc. before drawing such a conclusion.

In some cases, the initial screening tool might indicate a certain propensity to spread flame, but the initial flame spread calculation might indicate that flame spread will not accelerate or spread to a certain distance away from the point of ignition. Again, this type of scenario needs to be evaluated by the engineer with consideration of numerous other contributing factors.

6.2 Flame Spread Screening Tool

A first analysis screening approach has been established to help identify what commonly used materials in passenger rails are likely to support flame spread at various heat fluxes or energy rates to the surfaces per unit area. Approaches like the b-parameter can be very helpful as a first analysis screening tool, as it takes small-scale test results (i.e., the cone calorimeter), and helps predict large-scale tests and models. The b-parameter is a flame spread parameter and will show a material's tendency to accelerate or decelerate flame spread at various heat fluxes. The b-parameter will be used as a screening tool, comparing a large range of materials likely to be found in passenger rails. If the b-parameter is greater than zero, the flame is predicted to accelerate and spread, but if the b-parameter is less than zero, the flame is predicted to decelerate and eventually extinguish itself.

The following equation utilizes fire parameters measured or derived from cone calorimeter results with the variables explained below. Detailed theoretical development of this equation is not included in this paper because it is not the intent of this study [20][21].

$$b = 0.01\dot{E}'' - 1 - \frac{t_{ig}}{t_{end}} \qquad \text{[Eq. 5]}$$

Where,

$\dot{E}''$ = Average heat release rate per unit area (kW/m²)

T_{ig} = Time to ignition in the cone calorimeter

t_{end} = The end measured time in the analysis. For the purposes of this study, t_{end} will be measured as the time to flame out, time when the HRRPUA < 50 kW/m², as further discussed below.

A key understanding here is that geometric stability is extremely vital for accurate cone calorimeter results. Instability can result in skewed and inappropriate results. The governing equations behind these tests assume that the geometries remain stable throughout time. Highly expanding and geometric deformations during tests is a phenomenon that is physically observed and reported in the test notes. Materials of the sort will be noted and not included in this b-parameter study.

HRRPUA values were derived from cone calorimeter results and later graphed independently. An average HRRPUA is later determined for use in the b-parameter. In general, all materials behave differently in these tests; thus, each material must be analyzed independently, comparing the different tests at a variety of heat fluxes. As an example of the use of this tool, Figure 15 shows determined average HRRPUA values based on test results for a common fiber-reinforced plastic (FRP) material with a gelcoat surface.

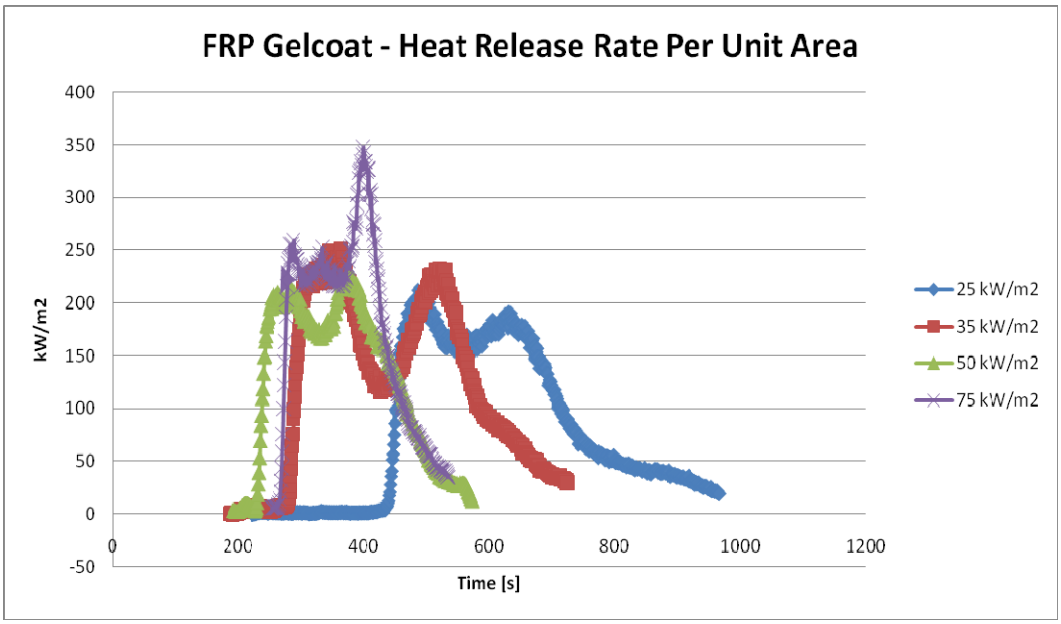

Figure 15. FRP Gelcoat – Combined Cone Calorimeter Results

While general observations (i.e., maximum HRRPUA, t_{ig}, $t_{flameout}$) can be made about the material from these graphs at the various heat fluxes, further analysis needs to be conducted while calculating the b-parameter.

A HRRPUA graph for each tested heat flux will help develop HRRPUA averages for various time scales as well as depict the appropriate time scale or length of time for each test. Similar to the skewed tests resulting from geometric instabilities, cellular flames and/or long tail like results at the end of tests, can also affect the outcome and values generated. Cellular flames, which are physically observed and recorded during each cone calorimeter

test, often represent instable flames that often flash during tests. Long tail like results at the end of cone tests is due to non-uniform or edge burning that result in extended values and times. This tail-like observation can further lead to lower HRRPUA averages. Due to the b-parameter dependence on uniform burning from cone tests, this requires individual consideration.

To account for these inefficiencies, each test must be independently analyzed. Figure 16 below, shows the HRRPUA values throughout the test with labeled t_{ig}, $t_{cellular}$, $t_{HRRPUA < 50\ kW/m^2}$ and $t_{flameout}$. When the time scale is shortened from t_{ig} to the time where the HRRPUA becomes cellular, or less than 50 kW/m², different HRRPUA averages can be obtained.

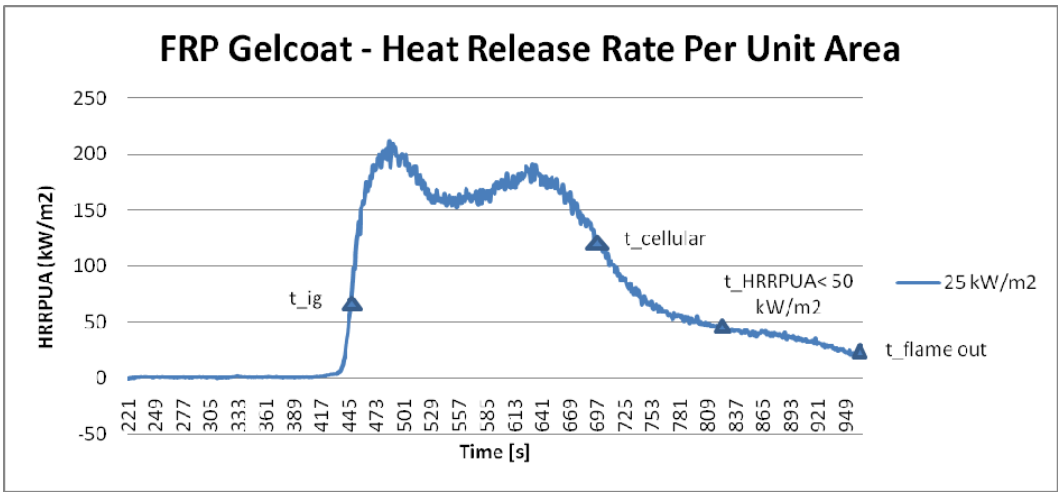

Figure 16. FRP Gelcoat - 25 kW/m² Cone Calorimeter Results

For each of these ending times, an average HRRPUA must be calculated. To do this, the area underneath the curve is obtained via integration. The area under the curve upon ignition to a specified time results in the total or summed HRRPUA. This is further shown in Figure 17.

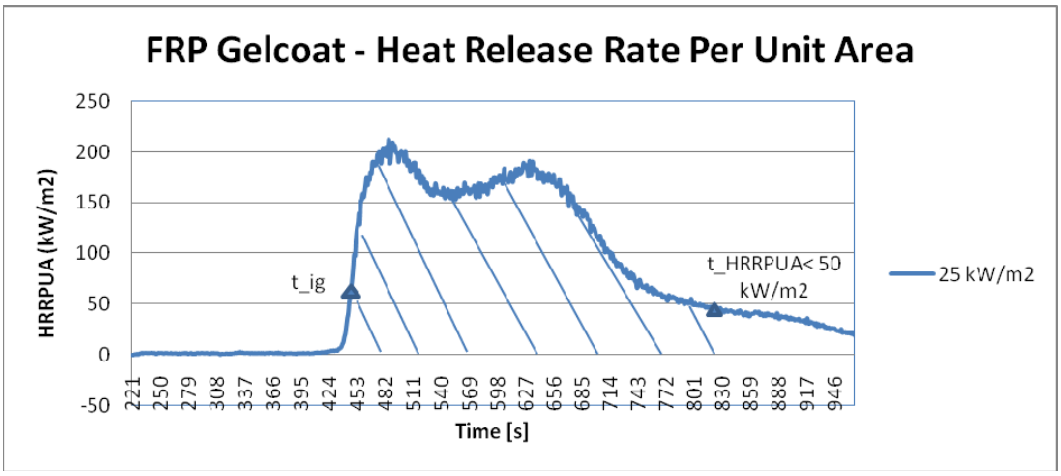

Figure 17. FRP Gelcoat - 25 kW/m² Summed HRRPUA

Derived cone calorimeter results for FRP Gelcoat, at a heat flux of 25 kW/m², gives a sum HRRPUA of 49,900 kW/m², from ignition time to the time when the HRRPUA becomes less than 50 kW/m². Dividing the HRRPUA sum by the time of this analysis, 354 seconds, gives an average HRRPUA of 141 kW/m².

This method of finding the average HRRPUA is undertaken for every material over a wide range of heat fluxes as obtained from an assortment of tests. Table 5 shows derived test results for heat fluxes at 25, 35, 50, and 75 kW/m².

Table 5. FRP Gelcoat – HRRPUA Values

FRP Gelcoat - HRRPUA Values (kW/m°)			
25 kW/m²		**35 kW/m²**	
$t_{cellular}$		$t_{cellular}$	
Sum HRRPUA	43,200	Sum HRRPUA	51,600
Average HRRPUA	167	Average HRRPUA	186
$t_{flame\ out}$		$t_{flame\ out}$	
Sum HRRPUA	55,900	Sum HRRPUA	62,400
Average HRRPUA	108	Average HRRPUA	143
$t_{HRRPUA < 50}$		$t_{HRRPUA < 50}$	
Sum HRRPUA	49,900	Sum HRRPUA	60,500
Average HRRPUA	141	Average HRRPUA	157
50 kW/m²		**75 kW/m²**	
$t_{cellular}$		$t_{cellular}$	
Sum HRRPUA	40,900	Sum HRRPUA	39,400
Average HRRPUA	183	Average HRRPUA	243
$t_{flame\ out}$		$t_{flame\ out}$	
Sum HRRPUA	45,600	Sum HRRPUA	46,800
Average HRRPUA	140	Average HRRPUA	182
$t_{HRRPUA < 50}$		$t_{HRRPUA < 50}$	
Sum HRRPUA	43,600	Sum HRRPUA	45,800
Average HRRPUA	167	Average HRRPUA	196

After the average HRRPUA, t_{ig}, and t_{end} are measured, or derived from tests, the b-parameter value can be calculated from Equation 5. Table 6 shows b-parameter values for FRP Gelcoat at heat fluxes of 25, 35, 50, and 75 kW/m². The end of the experiment, t_{bo}, or time to burnout, was considered to be the time when the flame became cellular, actual flameout occurred, or the HRRPUA became less than 50 kW/m². Table 6 further illustrates that the b-parameter varies depending on the endpoint time. Because consistency is needed to use the b-parameter as an initial screening tool, the end point is considered to be the time when the HRRPUA becomes less than 50 kW/m².

Table 6. FRP Gelcoat - B-Parameter Values

HRRPUA = 25 kW/m²		
$t_{cellular}=t_{bo}$	$t_{flame\ out}=t_{bo}$	$t_{HRRPUA < 50}=t_{bo}$
b = 0.041	b = -0.39	b = -0.15
HRRPUA = 35 kW/m²		
$t_{cellular}=t_{bo}$	$t_{flame\ out}=t_{bo}$	$t_{HRRPUA < 50}=t_{bo}$
b = 0.35	b = 0.034	b = 0.14
HRRPUA = 50 kW/m²		
$t_{cellular}=t_{bo}$	$t_{flame\ out}=t_{bo}$	$t_{HRRPUA < 50}=t_{bo}$
b = 0.30	b = -0.030	b = 0.19
HRRPUA = 75 kW/m²		
$t_{cellular}=t_{bo}$	$t_{flame\ out}=t_{bo}$	$t_{HRRPUA < 50}=t_{bo}$
b = 0.80	b = 0.30	b = 0.33

As previously explained, the b-parameter predicts the tendency of a flame to accelerate or decelerate. Therefore, Table 6 can be used as a first analysis screening tool in identifying a material's likelihood to accelerate and spread flame or simply extinguish itself. It is important to note that b-parameter values furthest from zero provide more definitive results comparing the b-parameter to realistic fire scenarios.

Based on the work done by Avila [22], representative uncertainty in b-parameter characteristics can be seen in Table 7.

Table 7. Uncertainty in b-parameter

Characteristic	Uncertainty
Heat release rate per unit area	45 kW/m²
Time to ignition	9 seconds
Burn duration	101 seconds
B-parameter	0.45 full scale (±0.225)

Classifying the time to burnout as the time when the HRRPUA is less than 50 kW/m² is generally a more conservative approach, because the long tail-like structure is cut off, raising the average HRRPUA and further increasing the b-parameter value. When the time to burnout is considered the time when the flame becomes cellular, on average, results in the highest b-parameter. This occurs because the time span is even shorter than that when the HRRPUA is less than 50 kW/m². The time to become cellular is often inconsistent and varies between tests, so only the time when the HRRPUA is less than 50 kW/m² will be used to compare all materials.

Figure 18, Figure 19, and Figure 20 show b-parameter data sets for various materials found in passenger rails.

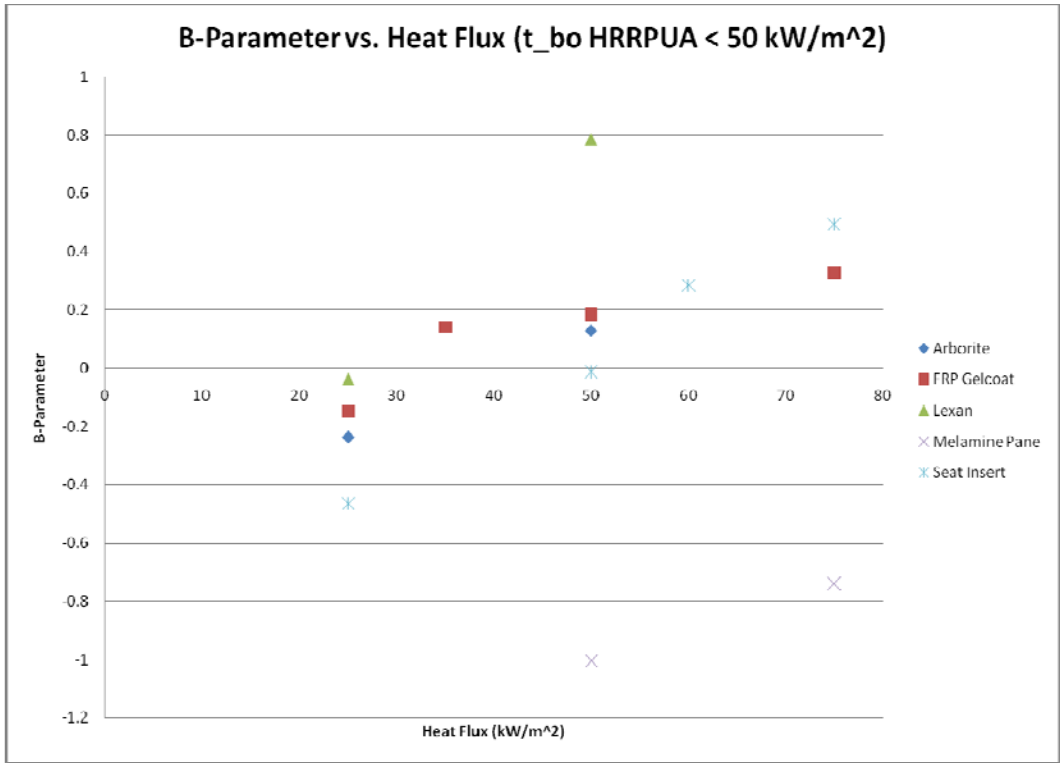

Figure 18. B-Parameter Data Set 1

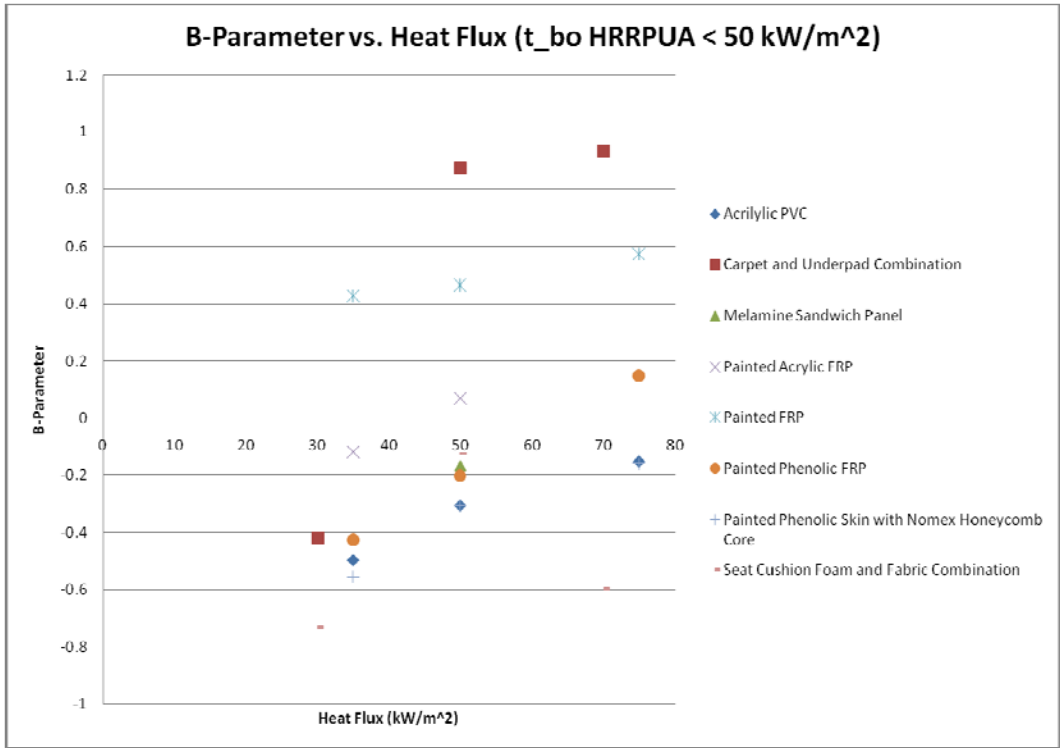

Figure 19. B-Parameter Data Set 2

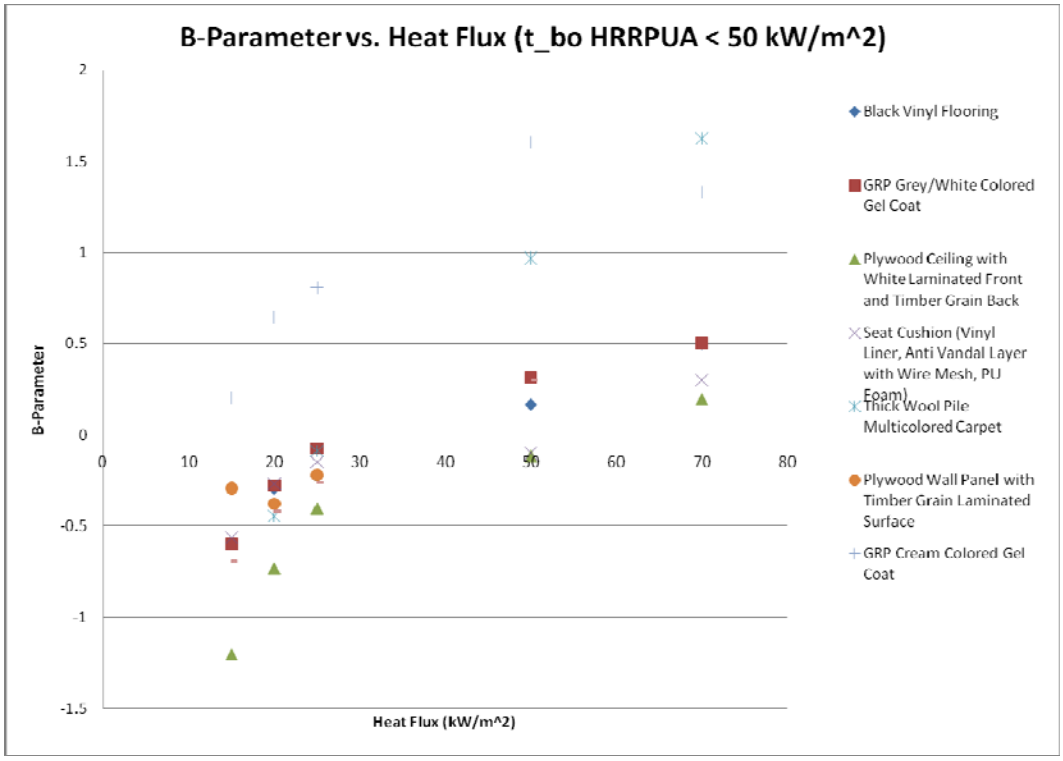

Figure 20. B-Parameter Data Set 3

Each data set has a wide range of materials tested at different heat fluxes. The b-parameter is calculated for each one of these tests and later represented in Figure 18, Figure 19, and Figure 20 above. Plotting an assortment of materials on the same axis shows which materials are predicted to accelerate or decelerate flame spread. Figure 20 shows that thick, wool pile, multicolored carpet will accelerate flame at lower heat fluxes than a plywood ceiling with a white laminated front and timber grain back. Assessing materials in this fashion will help compare materials that one currently has to materials used in other passenger rail vehicles.

6.3 Calculation of Initial Flame Spread

A simplified upward flame spread model was developed to represent likely flame spread that might occur in passenger and commuter rails. The work done by Mowrer and Williamson [23] guided the development of this model and associated equations. Flame spread is an exceptionally complex phenomenon, and it is important to understand its bounding conditions and assumptions associated. This model will focus on parameters measured in small-scale tests (i.e., cone calorimeter) and equations that model flame height, pyrolysis height, and burnout height. Velocity fronts (e.g., the flame spread velocity) can also be developed from this model.

HRR values can later be estimated and graphed throughout to better understand the energy involved. This paper will take a step by step approach for this process.

To better understand the science and analysis, a first look at the parameters involved is necessary. Figure 21 illustrates characteristics of upward flame spread [23]. The overall flame height, x_f, consists of the flame created on the wall by the external source fire and the flame extension up the wall. Pyrolysis is classified as the breaking down of materials into their vaporized form caused by an external heat sources. The pyrolysis height is

represented by x_p. When the fuel is considered spent or all used up, it can no longer support a flame and a burnout front develops, x_b.

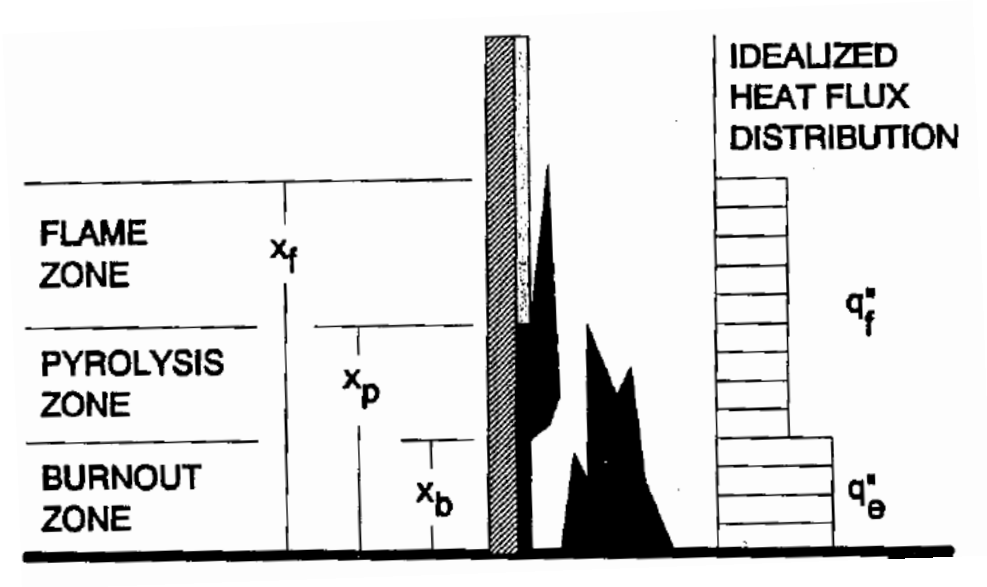

Figure 21. Upward Flame Spread Model

The initial source fire imposes an external heat flux on the vertical wall, q''_e. After the first exposed material is ignited, the flame extends up the wall emitting a flame heat flux, q''_f, to the virgin fuel. For the purposes of this model, preheating caused by convection and radiation from the soot and upper gas layer will be ignored. Conduction throughout the wall is also ignored, eliminating pre-heating of the wall by means of conduction.

The idealized heat flux distribution, in Figure 21, reveals the potential heat fluxes involved, assuming that the flame heat flux up the wall is constant. The external heat flux and flame heat flux, for the purposes of this study, will be considered the incident heat flux used in the cone calorimeter. This was deemed a reasonable approximation for the one-dimensional flame spread model for the incident heat flux in the cone calorimeter includes the flame formed in the cone.

Mowrer and Williamson [23] illustrate that the flame spread rate can be shown by the advancement of the pyrolysis front:

$$V_p = \frac{x_f(t) - x_p(t)}{t_f} \qquad \text{[Eq. 6]}$$

The characteristic flame spread time, t_f, is identified as the time to ignition from each of the cone calorimeter tests. This time to ignition is physically observed and recorded for each test at a range of heat fluxes (e.g., 25, 35, 50, and 75 kW/m²). This method assumes that the forwarding heating zones for each of these tests is 25, 35, 50, and 75 kW/m², respectively. Obtaining t_f directly from cone data further simplifies the model by neglecting parameters such as the temperature at ignition, $T_{ignition}$, and thermal inertia, $k\rho c$.

Once burnout initiates, Mowrer and Williamson [23] illustrate that the rate of fuel burnout can be shown by:

$$V_p = \frac{x_p(t) - x_b(t)}{x_{bo}} \quad \text{[Eq. 7]}$$

From these initial conditions, a crucial task is dividing the model into near field and far field zones.

The near field zone will comprise of the source fire with its initial heat flux and geometric configuration. The heat flux will represent the time period from the source ignition, t_{ig}^s, to the source burnout time, t_b^s. The characteristic geometry will consider the height and width of the initial source fire, x_{poh} and x_{pow}, respectively. This model assumes that initial ignition is based on the source fire.

The far field zone will comprise of the flame zone heat flux with the parameters to follow. The time to flame, t_f, based on the forward zone heat flux, is taken directly from the cone calorimeter. The far field zone will also consider $\dot{E}''$ and t_{bo} based on the pyrolysis zone heat flux. The losses from the forward heating zone are not accounted for, and the pyrolysis zone flame heat flux is 20 kW/m² greater than the heat flux measurements from the cone calorimeter (e.g., a cone calorimeter test at a heat flux of 50 kW/m² will result in a 70 kW/m² pyrolysis zone flame heat flux). As a simplified approach, t_b^s and t_{bo} are considered to be the same value, taken as the burnout time observed in the cone calorimeter. Further analysis on this relationship needs to be conducted.

Mowrer and Williamson [23] further integrate their governing equations to show the pyrolysis height, x_p, and the flame height, x_f, with the following equations and limitations:

x_p:

$t < t_{bs}$: $$x_p = x_{po} \exp\left[(k_f \dot{E}'' - 1)\frac{t}{t_f}\right] \quad \text{[Eq. 8]}$$

Limitations: $x=x_{po}$ at $t=0$ and $x=x_p$ at $t=t_f$

$t > t_{bs}$: $$x_p = (x_{p1} - x_{po}) \exp\left[\left(k_f \dot{E}'' - \frac{t_f}{t_{bo}} - 1\right)(t - t_b)/t_f\right] + x_b \quad \text{[Eq. 9]}$$

Limitations: $(x_p - x_b) = (x_{p1} - x_{po})$ at $t=t_b$ and $(x_p - x_b) = (x_p - x_b)$ at $t=t_f$

x_f:

$t < t_{bo}$: $$x_f = k_f \dot{E}'' x_p \quad \text{[Eq. 10]}$$

Limitations: Representative flame height based upon linearized flame length approximation [21][24][25].

$t > t_{bo}$: $$x_f = (k_f \dot{E}'')(x_p - x_b) + x_b \quad \text{[Eq. 11]}$$

Limitations: Representative flame height based upon normalized flame length.

Where:

x_{p1}= Pyrolysis height at t_b^s.

k_f= Correlating factor used to define the flame length ahead of the pyrolysis zone [23]. It is further suggested to use a value of approximately 0.01 m^2/kW [21].

E'' = The total heat release rate, HRR, or energy released during the cone calorimeter test.

$\dot{E}''$ = The average HRR, for the purposes of this study, measured from the cone calorimeter test.

Combining Equation 6 and Equation 9 result in:

$$\frac{dx_p}{dt} = (x_{p1} - x_{p0}) exp\left[\left(k_f \dot{E}'' - \frac{t_f}{t_{b0}} - 1\right)(t - t_b^s)/t_f\right] t_{b0}^{-1} \quad \text{[Eq. 12]}$$

Rearranging Equation 12 and combining constants yields:

$$\frac{dx_p}{dt} = C_2 exp[C_1 (t - t_i^s)] \quad \text{[Eq. 13]}$$

Where,

$$C_1 = (k_f \dot{E}'' - \frac{t_f}{t_{b0}} - 1) t_f^{-1} \quad \text{[Eq. 14]}$$

$$C_2 = \frac{x_{p1} - x_{p0}}{t_{b0}} \quad \text{[Eq. 15]}$$

Integrating Equation 13 results in the burnout height at any time:

$$x_b = \left(\frac{C_2}{C_1}\right)(exp[C_1(t - t_b^s)] - 1) + x_{p0} \quad \text{[Eq. 16]}$$

It is important to note when V_b is larger than V_p (i.e., the burnout front, x_b, is increasing at a greater rate than the pyrolysis front (x_p), a decelerating flame spread rate reducing the pyrolysis length, x_p-x_b, as a function of time.

Once the fundamental equations and bounding conditions were established, a model is created to demonstrate how these parameters relate to one another and how they change over time. To do so, initial fire characteristics need to be established. It is important to note that the aforementioned flame spread along the wall is concurrent flow flame spread which is considered one-dimensional, while the actual assumed flames for the model are two-dimensional in terms of a planer flame orthogonal to the wall. Special attention needs to be brought to this while developing this model into heat release rates.

To implement concurrent flame spread into representative HRR curves, particular attention needs to be brought to the overall pyrolysis and burnout areas. Developing burning area up the vertical wall is relatively easy, because only the source fire width is required. This of course neglects lateral spread up the wall until representative T-shape spread is incorporated, illustrated in Figure 22. T-shape flame spread depth can be assumed to be 0.08H, where H is the ceiling height [26]. Depending on the given scenario, the area underneath the ceiling needs to be incorporated if the ceiling is comprised of a combustible lining. Flame spread on ceilings is incorporated via representative semi-circles. Figure 22 illustrates representative pyrolysis and burnout development for a given scenario, represented by red and black, respectively.

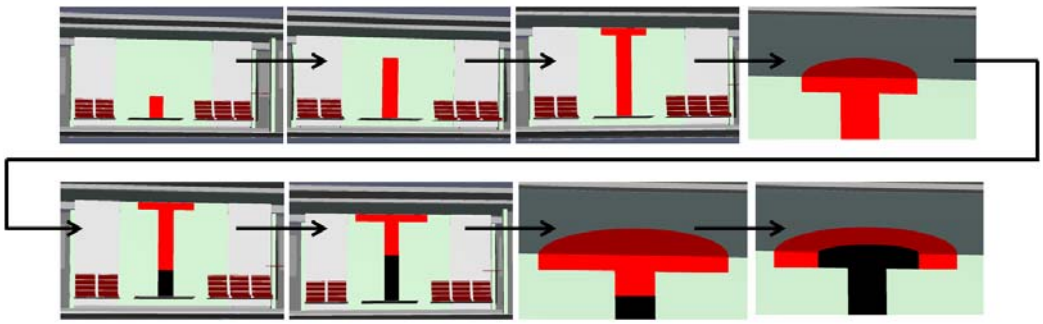

Figure 22. Representative Flame Spread

HRR values are established using, x_p-x_b, with the following:

For $X_p < H$ and $X_b < H$:

$$HRR\ vs.time = (x_p - x_b) * x_{pow} * \dot{E}'' \quad \text{[Eq. 17]}$$

For $X_p > H$ and $X_b < H$:

$$HRR\ vs.time = \left[(H - x_b)x_{pow} + 2D(x_p - H) + \frac{\pi}{2}\left(\frac{x_{pow}}{2} + (x_p - H)\right)^2\right]\dot{E}'' \quad \text{[Eq. 18]}$$

For $X_p > H$ and $X_b > H$:

$$HRR\ vs.\ Time = \left[2D(x_p - x_b) + \frac{\pi}{2}\left(\frac{x_{pow}}{2} + (x_p - H)\right)^2 - \frac{\pi}{2}\left(\frac{x_{pow}}{2} + (x_b - H)\right)^2\right]\dot{E}'' \quad \text{[Eq. 19]}$$

Where,

x_{pow}= Initial source fire width

H = Ceiling height

D = 0.08H (Representative T-shape depth)

Initial fire characteristics are developed through initiation fire scenarios (i.e., the fire geometry height and width, the length of time for this source fire, t_{bs}, as well as the imposed heat flux to the wall from the fire). For the purpose of this study, both small and large representative initiation fire scenarios are analyzed using FRP Gelcoat, with representative negative and positive b-parameter, respectively. This example utilizes cone calorimeter results for FRP Gelcoat at a heat flux of 25 and 50 kW/m².

The small initiation fire scenario is representative of a waste paper basket with a HRR of approximately 40 kW [8]. This is a reasonable scenario for approximation, because waste paper baskets tend to comprise of crumpled up paper, debris, and other miscellaneous trash that is likely found to be found on a passenger rail. An overall geometry of 0.5 x 0.3 meters (H x W) is assumed for a waste paper basket fire, with an incident heat flux of 25 kW/m² based on a 40 kW fire directly adjacent to the wall.

The larger initiation fire scenario is representative of 0.5 liters of gasoline on vinyl flooring with a HRR of approximately 400 kW [8]. This scenario is more likely of intentional circumstances with an arsonist carrying volatile substances. The overall geometry of this scenario is determined to be 1.0 x 0.6 meters (H x W), but subject to change based on the situation. With a HRR approximated at 400 kW, there is likely to be an incident heat flux of 50 kW/m² to the adjacent wall.

Both fire scenarios are analyzed in a rail vehicle with a three meter high wall and a three meter wide ceiling.

Table 8. Initiation Fire Characteristics for FRP Gelcoat

Scenario	Heat Flux (kW/m^2)	t_{bs} (s)	x_{p0h} (m)	x_{p0w} (m)	$\dot{E}''$ (kW/m^2)	$\dot{E}$ (kW)	t_f (s)
Small Fire	25	801	0.5	0.3	141	49,919	447
Large Fire	50	507	1	0.6	167	43,604	246

Incorporating these parameters into the model yields the flame spread zone heights illustrated in Figure 23 and Figure 24:

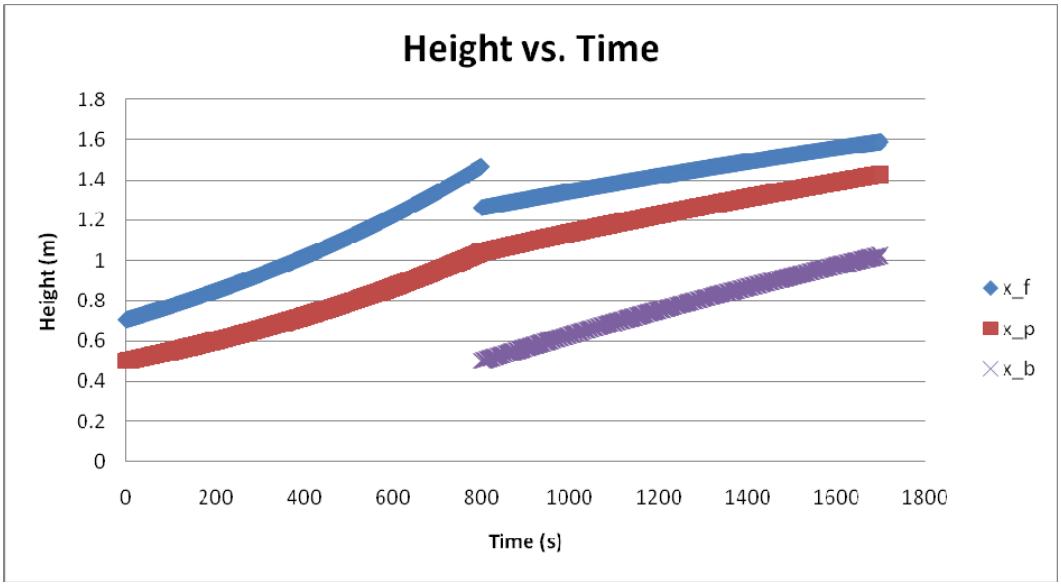

Figure 23. FRP Gelcoat - Upward Flame Spread Zone Heights (m) with Decelerating Flame Spread (Negative B-Parameter)

The large drop in flame height at 800 seconds is the result of the initial burnout of the first materials ignited. Figure 23 shows that the distance between the pyrolysis height and the burnout height, x_p-x_b, decreases over time indicating that there is a decelerating flame spread. This further holds true, because the calculated b-parameter is -0.15, also representing a decelerating flame spread for FRP Gelcoat at a heat flux of 25 kW/m².

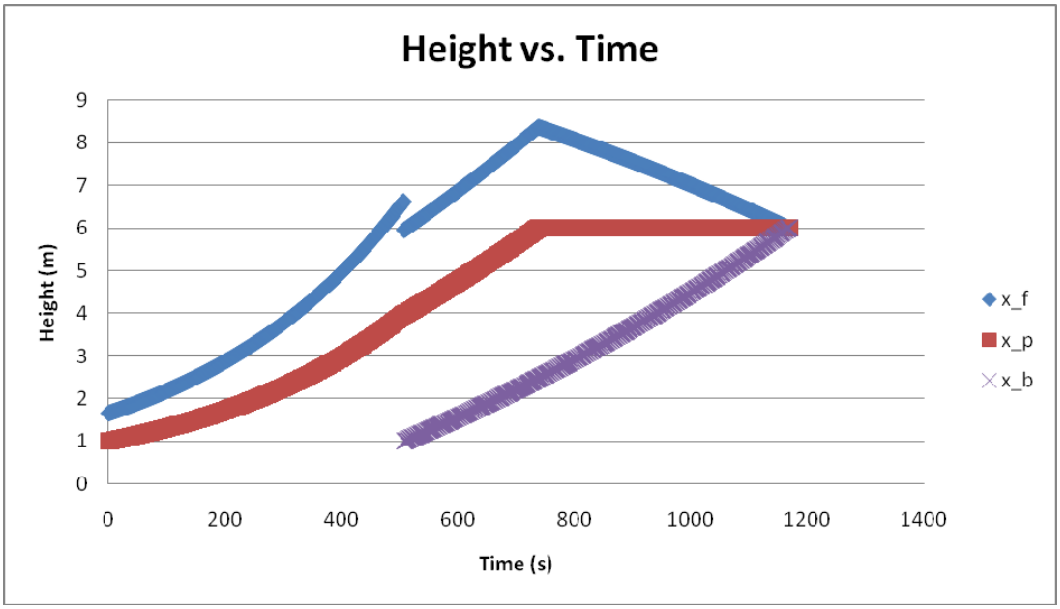

Figure 24. FRP Gelcoat - Upward Flame Spread Zone Heights (m) with Accelerating Flame Spread (Positive B-Parameter)

A large drop in the flame height is also illustrated in Figure 24, when the source fire burns out at 500 seconds. Figure 24 shows that the distance between the pyrolysis height and the burnout height, x_p-x_b, increases over time indicating that there is accelerating flame spread. With this, the pyrolysis height, x_p, reaches steady state around 700 seconds, indicating that the pyrolysis front has spread over all of the material. This condition would not hold true if there was an infinite amount of material. This scenario has a positive b-parameter of 0.19, at a heat flux of 50 kW/m².

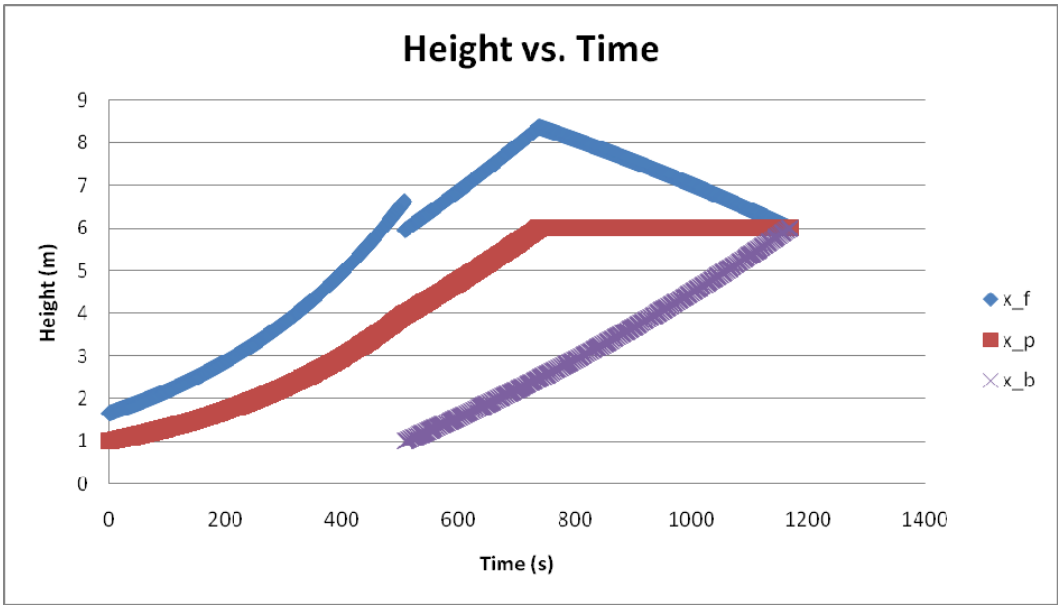

Figure 25. FRP Gelcoat - Calculated HRR (kW) Values for Decelerating Flame Spread

Figure 25 assumes that t_0 equals t_{ig} for the FRP Gelcoat on the wall. The peaking HRR, 0-800 seconds, represents flame spread before initial burnout. At 800 seconds, the initial materials burning diminish, greatly decreasing the HRR value. From 150 seconds, the HRR decreases due to a decelerating flame spread. The HRR trend significantly changes, because the source fire and initial materials ignited extinguish resulting in a flame front that can no longer sustain itself.

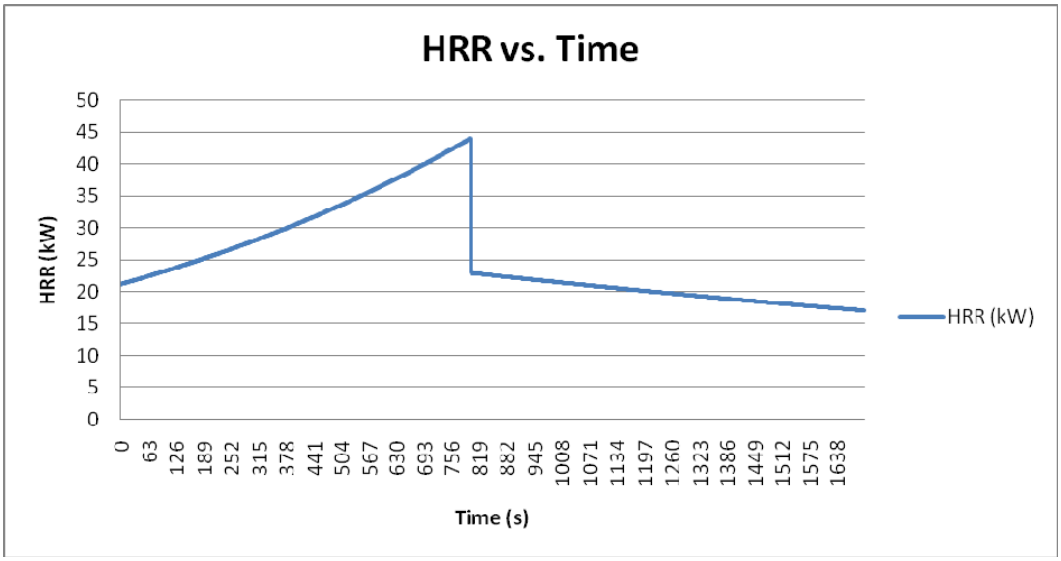

Figure 26. FRP Gelcoat - Calculated HRR (kW) Values for Accelerating Flame Spread

Figure 26 represents HRR characteristics for accelerating flame spread. The accelerating flame spread gives an exponentially increasing HRR value over time. At around 750 seconds, the HRR suddenly changes as the pyrolysis front has reached the end of available material or geometric constraints. With this, the pyrolysis front ceases forward progress, as

the burnout front continues to advance, decreasing the pyrolysis zone, x_p-x_b. The decreasing pyrolysis zone results in a decreasing HRR.

An accelerating flame spread creates great risk in the sense that the overall energy or HRR value can become unacceptably high fairly quickly. For this reason, it is important to analyze large assortments of materials at various heat fluxes found in passenger rails. These HRR values can be further utilized in models such as the Fire Dynamics Simulator (FDS) to represent the amount of energy released in a wide range of scenarios.

6.4 Fire Modeling

Computer fire modeling has been used by the fire protection engineering community since the late 1970's. With the advent of simple "zone" fire models such as FIRST [27] and CFAST [28] during the 1980's, fire model usage for forensic fire reconstruction and building design purposes became increasingly common. These models were relatively simple and could provide information about quantities such as temperature or smoke obscuration averaged over large volumes such as the "upper layer" in a compartment fire. Due to the limitations associated with computer processor speed and memory storage capacity, more comprehensive computational fluid dynamics (CFD) fire models were not practical for general usage until the late 1990's or the early years of this century.

Today, CFD-based fire modeling is used extensively worldwide for both building design and post-fire investigation. This was made possible by the rapid growth of computer power and storage combined with the public release of a free CFD-based fire model (Fire Dynamics Simulator [29][30]) in 2000. Although using CFD to model heat and smoke transport in buildings is now standard practice in the fire community, fire growth modeling to predict the heat release rate of a growing fire has not yet been widely applied. Rather, most practical applications of CFD fire models involve calculating the consequences or effects of a particular fire (characterized by a predetermined heat release rate history) on the space under consideration. Fire spread is not calculated in the simulation, rather it is prescribed by the user and typically design fires are idealized using *t*-squared fire growth relations. In this case, the CFD model does not calculate fire growth and flame spread, but simply tracks the evolution of smoke and heat through a building.

Although fire growth modeling has not yet been widely applied, there is substantial and growing interest in using first-principles computer modeling to predict real-scale fire behavior from small-scale fire test data. To date, it has been used mostly as a research tool and for calculating flame spread in simple geometries [31]. Specialized fire growth models have been developed for simulation of real scale fire tests [32][33], but these models lack generality and can usually be applied only to a particular geometry and ignition scenarios. NIST's freely available Fire Dynamics Simulator CFD code [29] (FDS) contains the basic physics necessary for fire growth modeling in general geometries, yet the extensive model validation literature survey conducted by NIST [30] identifies only four literature sources where the FDS code was used to predict flame spread in real scale, plus four studies of room fire growth. It was also noted that the capabilities of FDS to model flame spread are limited.

For these reasons, there is not yet any consensus in the fire protection community as to the "correct" values of model parameters related to fluid mechanics, combustion, and heat transfer in fire growth modeling. Furthermore, each material's fire behavior must be represented by a set of material properties that describe that particular material's reaction to fire. Although there are no direct tests to measure these properties, they can be estimated from existing small-scale fire test data. Since all of these factors create an inherent degree

of uncertainty, it is prudent to calibrate any model by comparing its predictions to fire test data, if possible.

6.4.1 Fire Model Description (NIST Fire Dynamics Simulator)

The NIST Fire Dynamics Simulator code (FDS) works by solving "conservation equations", which state mathematically that mass, momentum, and energy are conserved. In their most detailed form, the conservation equations are exact. FDS solves a simplified form of these governing equations that have come to be known as the "low Mach number combustion equations", first proposed by Rehm and Baum [15] at the National Bureau of Standards, now NIST (the developers of FDS). The inherent assumption is that velocities are small in comparison to the speed of sound (~340 m/s at standard temperature and pressure). This allows for considerable simplification of the conservation equations, making efficient solutions of the governing equations possible. The low Mach number assumption is appropriate for low-speed thermally driven flows such as those that occur during fire, but would not be appropriate where velocities exceed approximately 90 m/s.

In the FDS program, the space being simulated is broken into a large number of "cells" corresponding to a fixed region in space, and the conservation equations are solved for each cell. The end result is a detailed spatial and temporal description of the temperature, velocity, and species fields. Although the equations on which FDS is based are scientifically rigorous, the primary difficulty of fire modeling at the present time is limited computer power, stemming from the wide range of length and time scales involved in fires. Combustion occurs at length scales smaller than 1.0 mm, but bulk fluid flow occurs on length scales of 1.0 m or more. To put this into perspective, approximately 166 *billion* cells would be required to model the standard-sized fire test burn room (3.6 m by 2.4 m by 2.4 m) with a grid resolution fine enough to resolve the flame sheet (0.5 mm). Even on today's fastest multi-processor supercomputers, it is not possible to run such a large simulation.

Since all relevant length scales cannot be resolved on today's computers, several strategies have been developed. FDS belongs to a class of models that use Large Eddy Simulation (LES) to account for the effect of unresolved length scales. Phenomena that occur at length scales on the same order as the grid spacing, such as buoyant smoke transport and fluid flow, are directly calculated from the conservation equations. However, phenomena that occur at length scales smaller than the grid spacing, such as combustion and turbulent mixing, are approximated or modeled. The sub-grid scale models used by FDS out of necessity introduce several "model parameters", for which there is no widespread agreement as to how to select proper values. In this work, the values of these adjustable model parameters will be determined through a calibration exercise by finding the set of parameters that give optimal agreement between the model prediction and available experimental data.

7 Demonstration of Approach

This section provides an example of the application of the analysis approach proposed here to the assessment of the fire hazard of passenger rail vehicle interior materials.

7.1 Disclaimer

The case study documented here references generic materials and vehicle design parameters. Its purpose is to demonstrate the analysis methodology that has been proposed. It is not intended as a source for input data to support fire modeling or analysis. It is also not a formal evaluation of the types of materials discussed.

7.2 Scenario

As a demonstration of the analysis approach proposed here, consider the following scenario.

> An urban rail operator is adding a series of new vehicles to their subway system. Tunnel and station fire and life safety features (suppression, smoke exhaust, etc.) are not being upgraded, so the new vehicles must be designed with attention to the constraints of these fire and life safety systems. In particular, smoke control systems we designed to address a design fire scenario of no greater than 11 MW.
>
> The rail vehicle design team has narrowed the choice of interior wall and ceiling linings to two glass-reinforced plastic material options and wishes to understand the possible fire hazards associated with these. Full-scale fire tests of these materials in the vehicle installation are not possible within the design budget or schedule.

The materials being considered are labeled GRP A and GRP B for the purposes of this analysis. Because this report is not intended to draw conclusions or provide recommendations relative to these specific materials, further material property data is not presented here.

7.3 Analysis Process

The following process will be used to evaluate the proposed materials:

1. Determine material flammability characteristics through cone calorimeter testing. Expose materials to a range of heat fluxes.
2. Estimate flame spread behavior through spreadsheet analysis. Determine the B parameter for each material.
3. If final conclusions regarding the fire hazard of the proposed materials can be derived based on the calculated B parameters (i.e. one or both have strongly negative B parameters indicating no likelihood to spread flame) and there are not other fire hazard concerns (such as unique geometrical arrangements – as determined by the fire protection engineer), analysis is complete. If not, continue to as below.
4. Determine CFD model input parameters through application of a genetic algorithm analysis using the cone calorimeter data.
5. Simulate various design fires within the vehicle using CFD for each material. Model initial flame spread as a series of burners that together recreate the flame spread

behavior predicted by the spreadsheet analysis in Step 2 above. Model adjacent surface materials based on the results of the genetic algorithm analysis in Step 4.

6. Use CFD results to inform the material choice and to help understand the overall fire hazard associated with the vehicle.

The following subsections demonstrate this process.

7.4 Analysis

7.4.1 Cone Calorimeter Testing

Cone calorimeter tests were carried out according to ASTM and ISO standards. In addition, modifications were made to the apparatus to record specimen surface temperatures because these are required for determining CFD input parameters. The specimen holder was modified so that temperature measurements could be taken inside the sample (where possible) and on the back face of the sample. The top surface temperature of the sample was measured using an infrared camera mounted above the cone heating element.

The cone calorimeter was used to expose GRP A and GRP B to heat flux levels of 15, 20, 50, and 75 kW/m². The results of the 20 and 50 kW/m^2 tests are shown in Figure 27 through Figure 30.

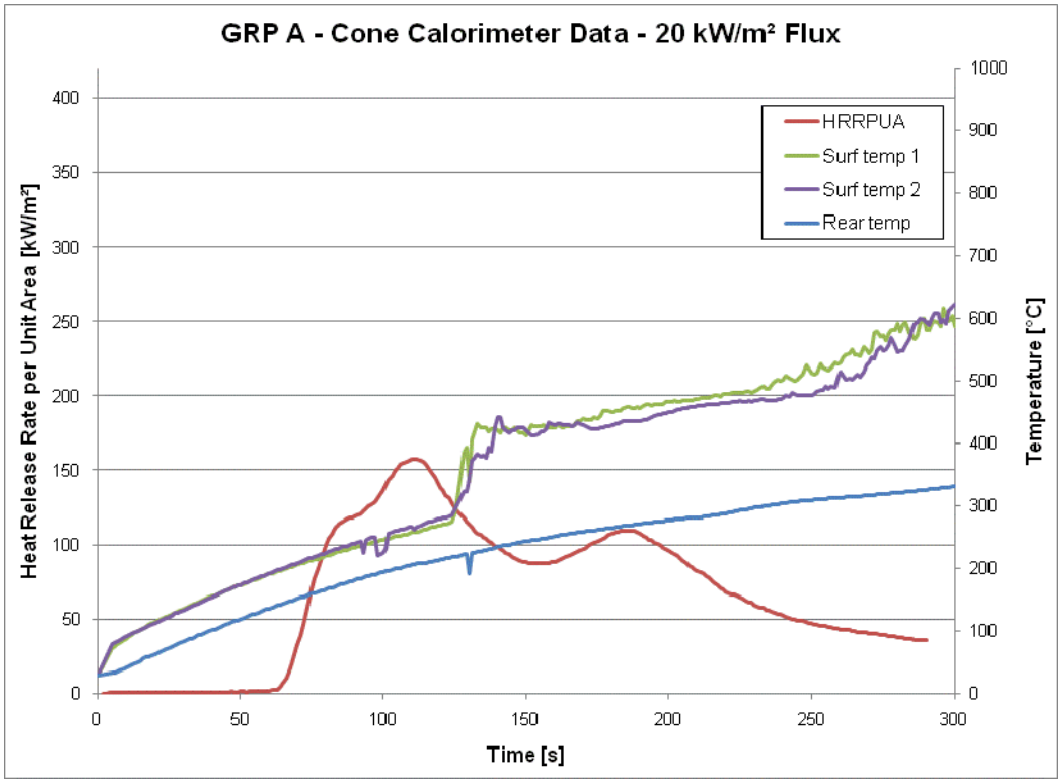

Figure 27. Cone Calorimeter Data – GRP A with 20 kW/m² Flux

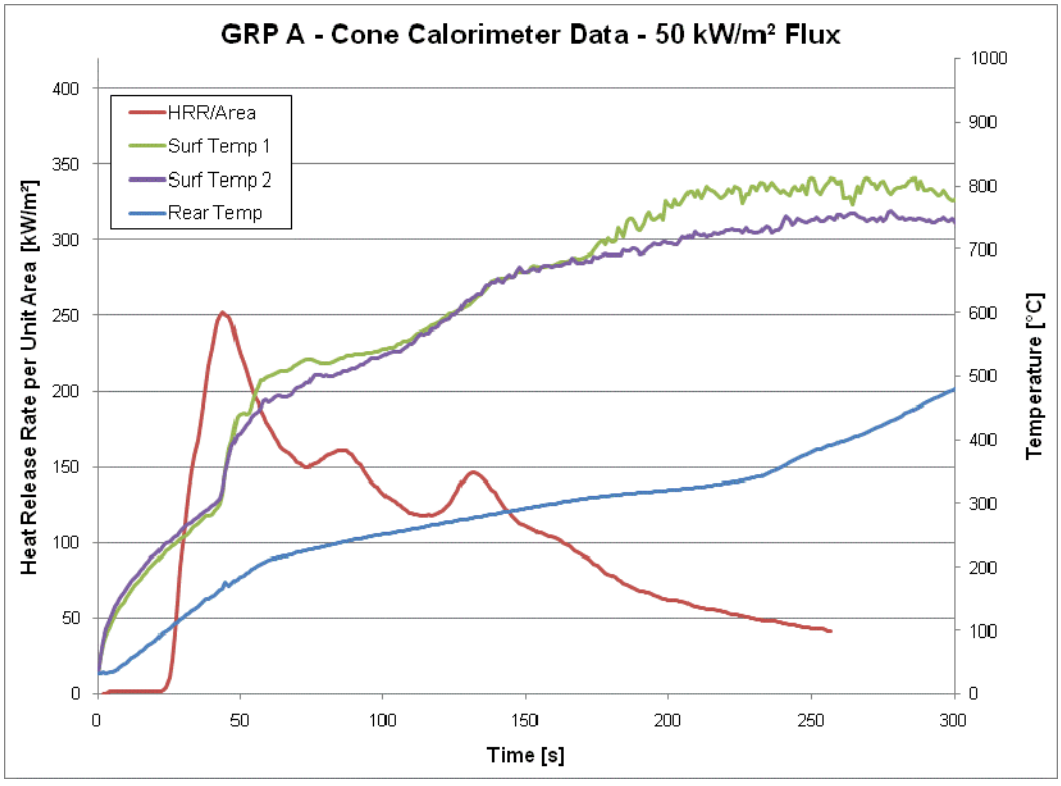

Figure 28. Cone Calorimeter Data – GRP A with 50 kW/m² Flux

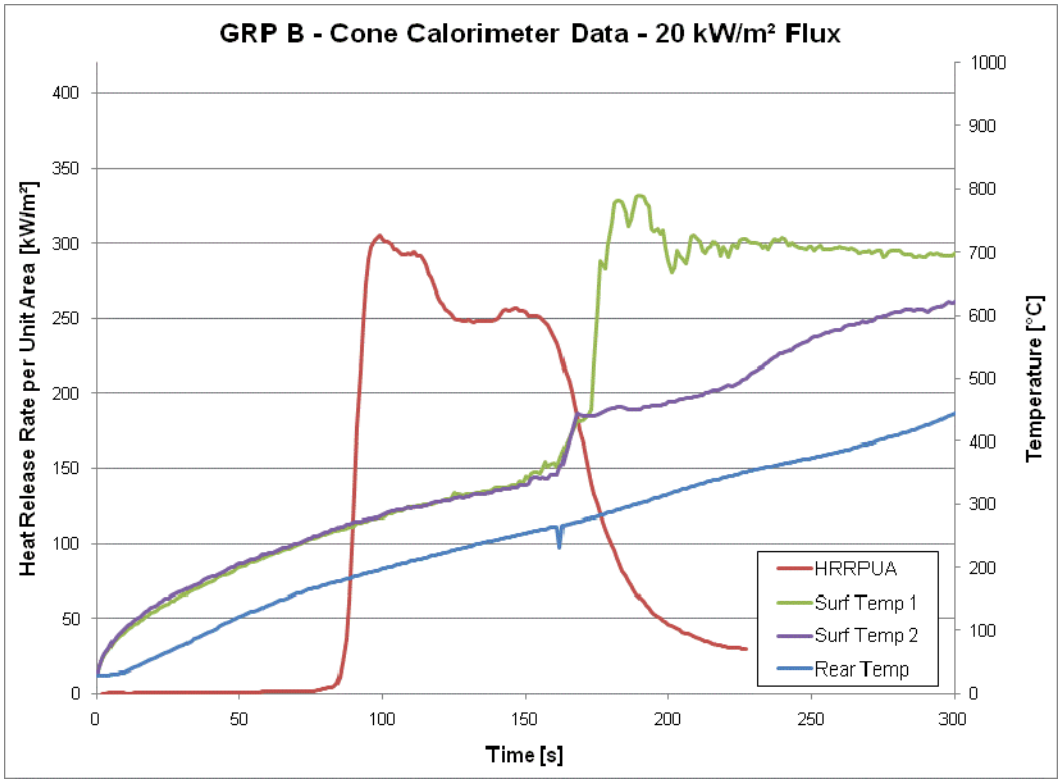

Figure 29. Cone Calorimeter Data – GRP B with 20 kW/m² Flux

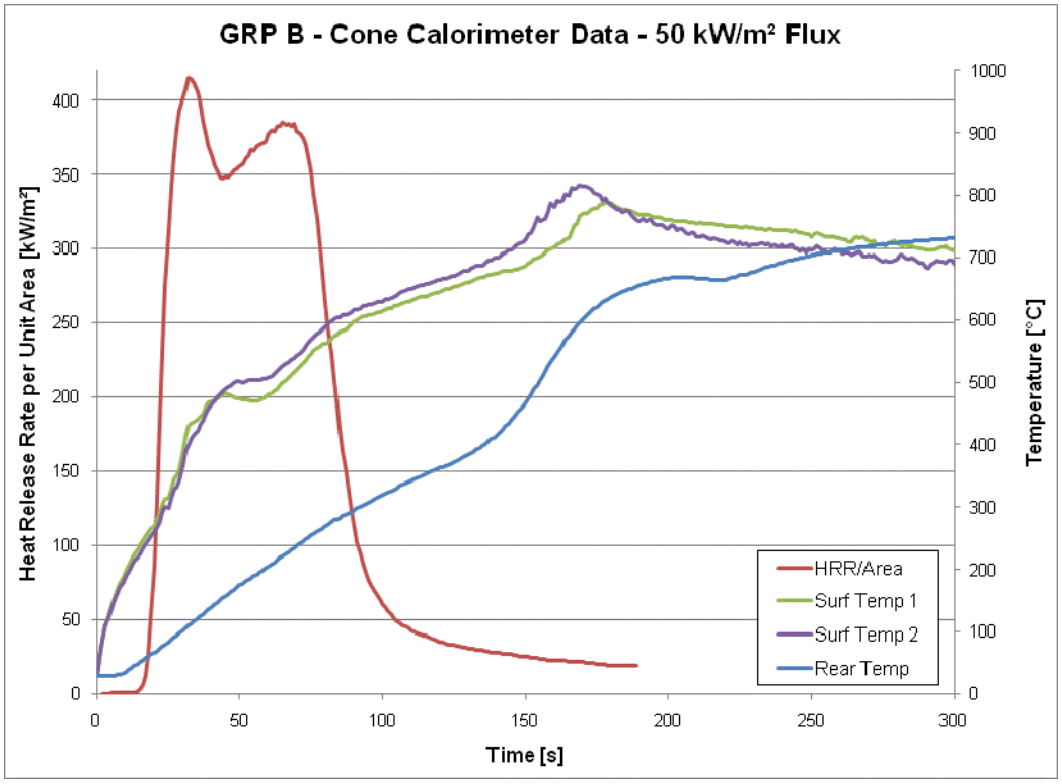

Figure 30. Cone Calorimeter Data – GRP B with 50 kW/m² Flux

7.4.2 B-Parameter Estimation

Using the methodology discussed in Section 6, b-parameter values were determined for the two types of GRP for each heat flux level used in the cone calorimeter tests. The results of the b-parameter calculations are shown in Table 9.

Table 9. Calculated B Parameter Values

Material	Heat Flux (kW/m²)	B-Parameter
GRP A	15	-0.60
	20	-0.28
	50	0.31
	75	0.50
GRP B	15	0.20
	20	0.64
	50	1.60
	75	1.33

GRP B has positive b-parameter values for all heat flux levels, indicating that it has a tendency to spread flame. This is especially true given heat flux values in excess of 20, for which strongly positive b-parameter values are calculated. The b-parameter calculated for a heat flux exposure of 15 kW/m^2 is not as definitive, and thus would likely warrant further review.

Unlike GRP B, GRP A exhibits negative b-parameters given a heat flux of 20 kW/m^2 or less. Even at a heat flux level of 75 kW/m^2, the b-parameter calculated for GRP A is less than that calculated for GRP B given a much lower heat flux (20kW/m^2).

Based on this analysis, it could be concluded that the installation of GRP A will most likely lead to less flame spread for a given initiating fire scenario than GRP B would. However, if heat flux levels greater than 20 kW/m^2 are possible, further analysis is required in order to understand the ultimate impact of these materials on the fire hazard of the vehicle.

7.4.3 Estimation of Initial Flame Spread

The output from the cone calorimeter tests was used to develop predictions of initial flame spread behavior using the methodology discussed in Section 7.4.3. Figure 31 and Figure 32 provide example results from this analysis. These show the positions of the flame front, pyrolysis front, and burnout front as a function time, as well as the predicted heat release rate curves for the two GRP materials given a heat flux of 50 kW/m².

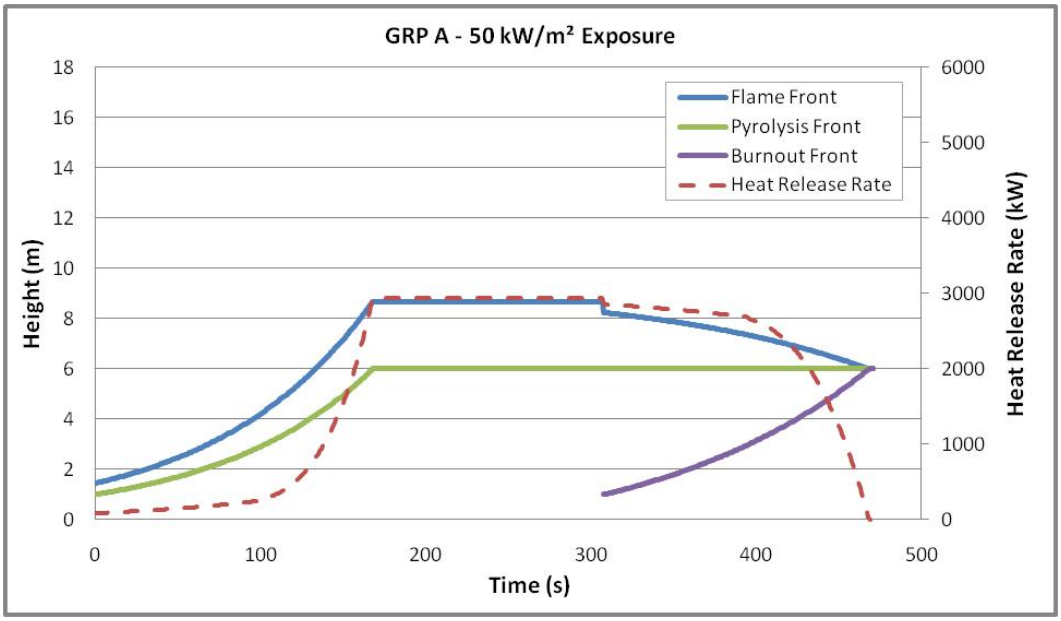

Figure 31. Flame Spread Analysis Results – GRP A with 50 kW/m² Exposure

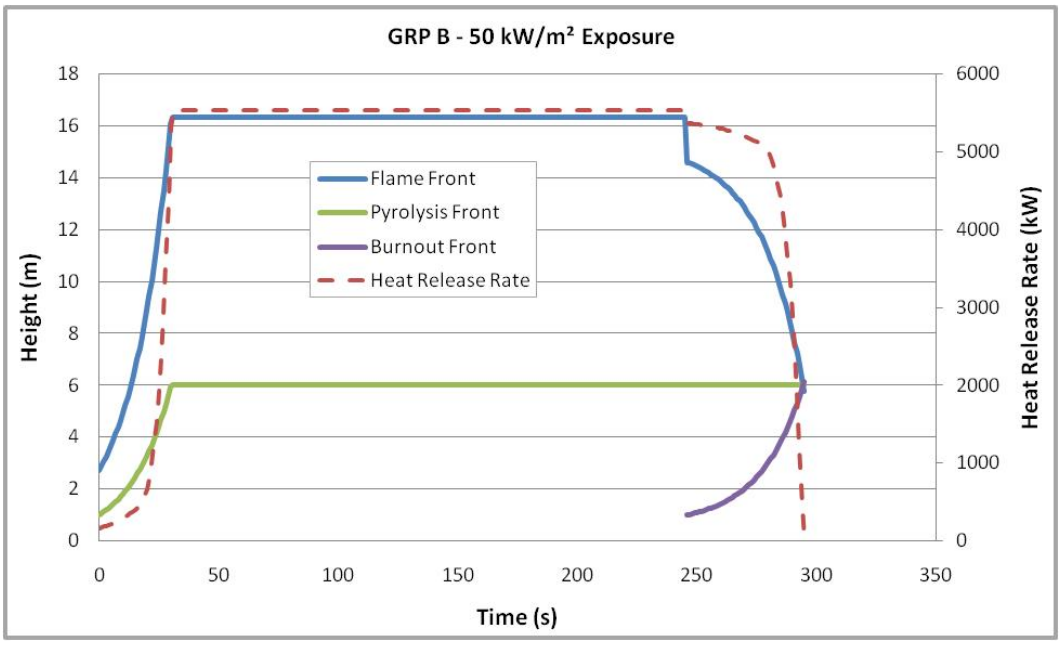

Figure 32. Flame Spread Analysis Results – GRP B with 50 kW/m² Exposure

Both materials support flame spread given a heat flux exposure of 50 kW/m². GRP A exhibits a lower calculated average heat release rate per unit area than GRP B, and thus the peak heat release rate for GRP A is lower than that of GRP B. The pyrolysis front for GRP B reaches the ceiling (at 3.0 m) and then the far side of the ceiling (at 6.0 m) more quickly than the pyrolysis front of GRP A does, thus indicating that, under these conditions, GRP B can be expected to spread flame more rapidly than GRP A.

While these results do indicate that GRP A will spread flame less rapidly than GRP B, they also indicate that both of these materials are likely to spread flame when subjected to certain levels of heat flux. Therefore, these results are not sufficient to draw conclusions

regarding the conformance of these materials to the performance criteria defined by the stakeholders. Further modeling is required to determine the global impact of this initial flame spread within the rail vehicle.

7.4.4 Determination of Material Input Parameters for CFD

The genetic algorithm approach discussed in Section 5.2.2 was used to determine input parameters for FDS based upon the data obtained through the cone calorimeter testing. The subsections that follow summarize the outcome of this work.

Appendix B provides the FDS input fields determined for these materials.

7.4.4.1 Surface Input Parameters

Surface input parameters in FDS are used to describe the composition of solid surfaces. The material or materials that constitute the surface are defined in this way, as is the condition directly behind the surface (i.e. air gap, insulation, etc.).

Table 10 lists the surface parameters determined through use of the genetic algorithm analysis for the two example materials being considered here.

Table 10. GRP Surface Input Parameters

Parameter	Input Values	
	GRP A	**GRP B**
Stretch Factor	1.000	1.000
Cell Size Factor	0.500	0.500
Material 1 Thickness	0.0027 m	0.0035 m
Material 1 Name	GRP_A_Virgin	GRP_B_Virgin
Material 1 Mass Fraction	1.000	1.000
Material 2 Name	GRP_A_Char	GRP_B_Char
Material 2 Mass Fraction	0.000	0.000
Back Boundary Condition	Insulated	Insulated
Shrinking Material	False	False
Initial Solid Temperature	27.0°C	27.0°C

In the table above, Material 1 represents the initial state of the surface (virgin, unburned GRP). Material 2 represents the state that remains after pyrolysis (char), and thus composes zero percent of the mass of the surface at the start of the simulation.

The parameters *cell size factor* and *stretch factor* allow the user to increase the numerical stability of the pyrolysis calculation. By setting cell size factor to 0.5, the surface mesh cells that are used to calculate heat transfer are reduced in size to half of the size calculated through a default rule in FDS. This rule bases the surface mesh cell size on the square root of the material's thermal diffusivity. Setting the stretch factor to 1.0 forces the surface mesh cells to be uniform in size.

7.4.4.2 Material Input Parameters – Virgin GRP

FDS uses material input parameters to describe the components of a solid surface. As discussed above, the surface input refers to the materials that compose the surface and distribute / orient them to represent the surfaces being modeled.

Material input parameters describe the thermal properties of the materials being modeled such that pyrolysis and flame spread can be calculated. They also specify the yields of fuel, water, and residue that occur when the material is heated. In the case of the GRP material being considered here, the residue is char.

Table 11 lists the material parameters determined through use of the genetic algorithm analysis for the virgin states of the two example materials being considered here.

Table 11. Virgin GRP Material Input Parameters

Parameter	Input Values	
	GRP A Virgin	**GRP B Virgin**
Density	1721.0 kg/m³	1312.6 kg/m³
Emissivity	0.864	0.867
Conductivity	See Figure 33	See Figure 33
Specific Heat	See Figure 34	See Figure 34
Absorption Coefficient	0.10E+7 /m	0.10E+7 /m
Residue	GRP_A_char	GRP_B_char
Pre-exponential Factor (A)	0.74E+9	0.23E+10
Activation Energy (E)	0.12E+6 kJ/kmol	0.13E+6 kJ/kmol
Exponent of Mass Fraction	1.210 /s	1.500 /s
Heat of Reaction	1636.1 kJ/kg	682.8 kJ/kg
Fuel Yield	0.400 kg/kg	0.544 kg/kg
Residue Yield	0.600 kg/kg	0.456 kg/kg
Steam Yield	0.000 kg/kg	0.000 kg/kg
Number of Reactions	1	1

The conductivity and specific heat of these materials change with temperature. The graphs in Figure 33 and Figure 34 show the temperature dependence of these parameters as predicted by the genetic algorithm analysis for the virgin GRP materials.

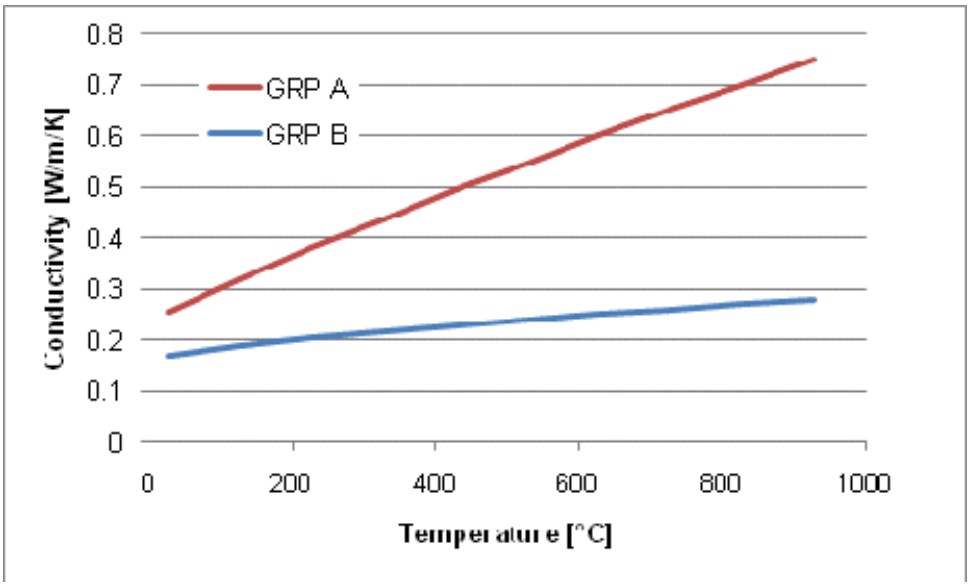

Figure 33. Virgin GRP Conductivity Temperature Dependence

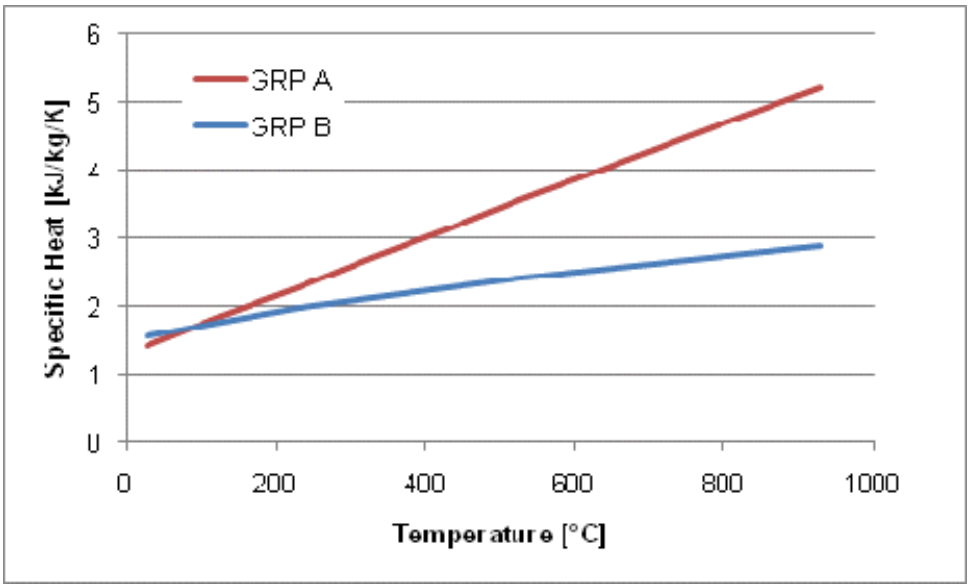

Figure 34. Virgin GRP Specific Heat Temperature Dependence

7.4.4.3 Material Input Parameters – GRP Char

Table 12 lists the material parameters determined through use of the genetic algorithm analysis for the char state of the two example materials being considered here.

Table 12. GRP Char Material Input Parameters

Parameter	Input Values	
	GRP A Char	GRP B Char
Density	1032.6 kg/m³	598.9 kg/m³
Emissivity	0.927	0.924
Conductivity	See Figure 35	See Figure 35
Specific Heat	See Figure 36	See Figure 36
Absorption Coefficient	0.10E+7 /m	0.10E+7 /m
Number of Reactions	0	0

The graphs in Figure 35 and Figure 36 show the temperature dependence of the GRP char materials' conductivity and specific heat as predicted by the genetic algorithm analysis.

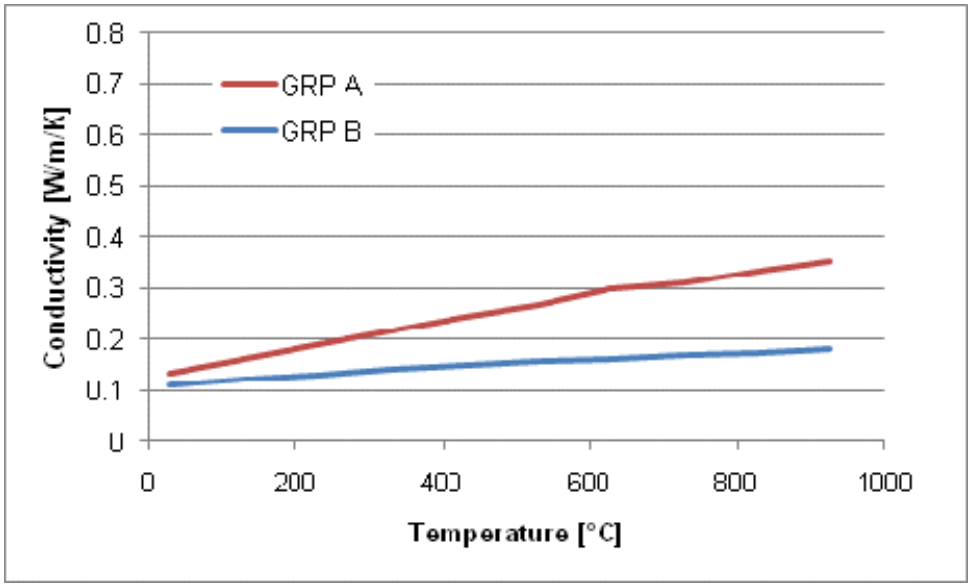

Figure 35. GRP Char Conductivity Temperature Dependence

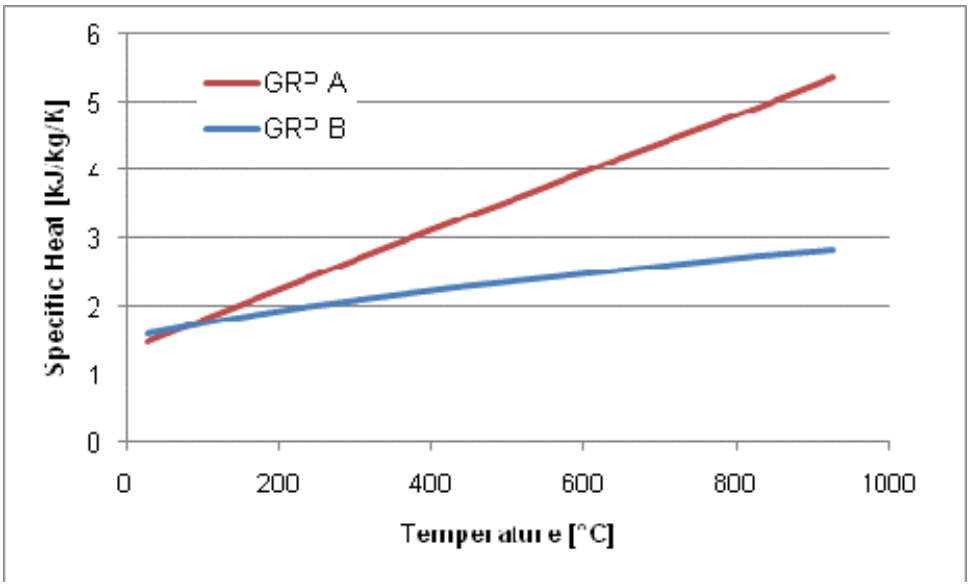

Figure 36. GRP Char Specific Heat Temperature Dependence

7.4.5 CFD Simulations

An FDS model of a typical subway car was developed to evaluate the impact of the two GRP materials. The figures below show this model.

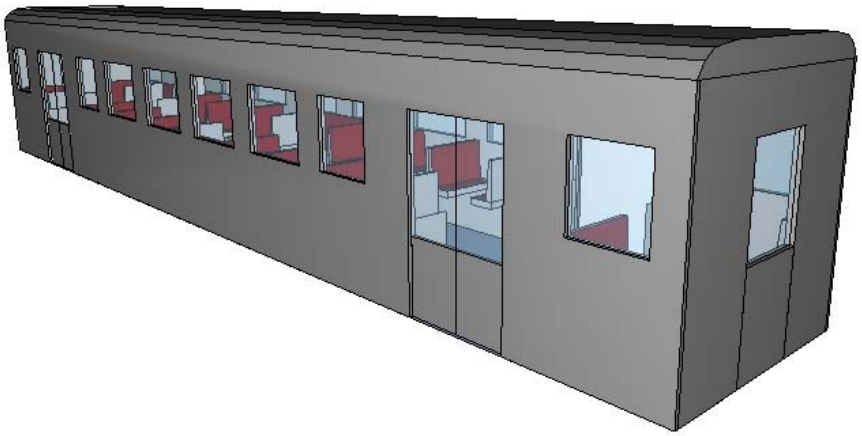

Figure 37. Exterior View of FDS Model

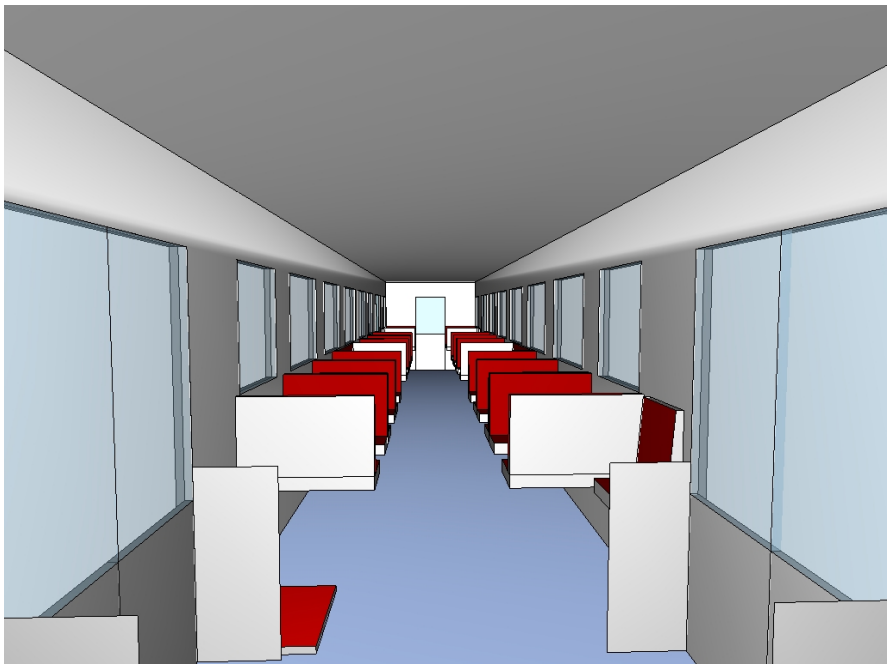

Figure 38. Interior View of FDS Model

7.4.5.1 CFD Model Materials

Within the FDS model, all wall and ceiling surfaces, including door interior linings, were composed of the GRP material being considered. Seats were assumed to be comprised of steel structures with plastic sides and back and carpet-like seat surfaces. The flooring was assumed to be a rubber-based flooring material. Since the seat and floor materials are not being evaluated here, the models evaluating GRP A and GRP B assumed the same seat and floor materials.

All windows were assumed to be glass. Breakage of windows was not modeled.

7.4.5.2 Ventilation Conditions and Station Effects

It was assumed that all doors on one side of the car were open during the modeled fire scenario. This represents a condition where the car is parked at a station with the doors on one side open. End car doors were assumed to be closed.

Effects of station geometry and fire protection systems (such as sprinklers and smoke control) were not modeled because the intent of the analysis was to evaluate the effect of different materials on overall fire size. The smoke was assumed to vent from the train to an infinite volume.

7.4.5.3 CFD Mesh Dimensions

WPI and Arup, in conjunction with the University of California at Berkeley, have conducted significant research regarding the sensitivity to predicted flame spread to computational grid dimensions [34]. This research indicates that for fire sizes and materials typical of passenger rail vehicles, flame spread is predicted well with a grid resolution of 5.0 cm. Computational grid cells smaller that 5.0 cm do not provide appreciably greater accuracy, but would require significantly greater computational resources and time to process.

The analysis discussed here used 5.0 cm grid cells throughout the vehicle model.

7.4.5.4 Fuel Properties

Table 13 lists the fuel reaction properties used in FDS to represent the GRP materials.

Table 13. GRP Reaction Properties

Property		Value
Heat of Combustion		11,000 kJ/kg
Soot Yield		0.096 g_{soot}/g_{fuel}
CO Yield		0.058 g_{CO}/g_{fuel}
Chemical Reaction	Carbon Atoms	2.1
	Hydrogen Atoms	2.0
	Oxygen Atoms	1.0

Further, the "ideal energy" function of FDS was disabled in order to force the analysis to account for CO, hydrogen, and soot yields.

7.4.5.5 Thermal and Fluid Boundary Conditions

The initial temperature for the ambient environment and all surface boundaries has been specified as 20°C.

The spread of smoke has been calculated using large eddy simulation (LES) techniques, in which the large-scale eddies are computed directly and the sub-grid scale dissipative process is empirically modeled. This means that the large-scale mixing taking place between the plume/smoke layer and the ambient air is computed directly through first principles by the CFD model.

7.4.5.6 Design Initiating Fire

For the purposes of this demonstration, a single initiating fire on the floor of a vehicle adjacent to a wall has been considered. An analysis of a proposed rail vehicle should include attention to a range of design fire scenarios.

Different combustible materials require different levels of incident heat flux in order to ignite. In some cases, the required heat fluxes may not be possible given credible design initiating fires. It is important to review the likely fires within the vehicle being studied in order to understand the hazards they present to the lining materials.

FDS was used to review incident (gauge) heat flux levels at a wall surface as a result of a range of fires located immediately adjacent to the wall and 0.3m (1.0 ft) from the wall. The results are shown in Table 14.

Table 14. Review of Heat Fluxes from Various Fire Sizes

Fire Size	Heat Flux: Fire Against Wall	Heat Flux: Fire 0.3m from Wall
500 kW	95 kW/m²	30 kW/m²
1000 kW	105 kW/m²	40 kW/m²
2000 kW	120 kW/m²	55 kW/m²
5000 kW	150 kW/m²	85 kW/m²

The materials being considered here have strongly-positive B parameter values when exposed to heat flux values on the order of 50 kW/m². Based on the above review of heat flux values, it can be concluded that when fuels are located immediately adjacent to a wall surface, wall material ignition can be expected to occur given fires on the order of 500 kW. If a stand-off or separation is provided such that combustible materials cannot be located within 0.3m from the wall, a larger total fire size is likely required in order to ignite the wall materials.

The CFD analysis has assumed that a 500 kW initiating fire occurs in contact with a wall of the vehicle.

A 500 kW fire representative of several bags of trash, and is slightly larger than the fire size resulting from a spill of 1.0 L of gasoline on a smooth flooring material, such as vinyl tiles [8].

7.4.5.7 Implementation of Initial Flame Spread in CFD Model

Initial ignition and flame spread on the wall materials in the FDS model were manually specified to match the predictions presented in Section 7.4.3. A series of burner surfaces with reaction properties as discussed in Section 7.4.5.4 were implemented in the model and included heat release rate growth and decay curves designed to recreate the total heat release rate and pyrolysis zone predictions determined through the initial flame spread analysis. These burners were sized and prescribed with individual heat release rate curves such that, at any given time, the extent of pyrolysis and the total heat release rate is equivalent to that predicted by the initial flame spread analysis.

Figure 39 and Figure 40 show how the heat release rates prescribed in FDS align with the curves calculated during the initial flame spread analysis.

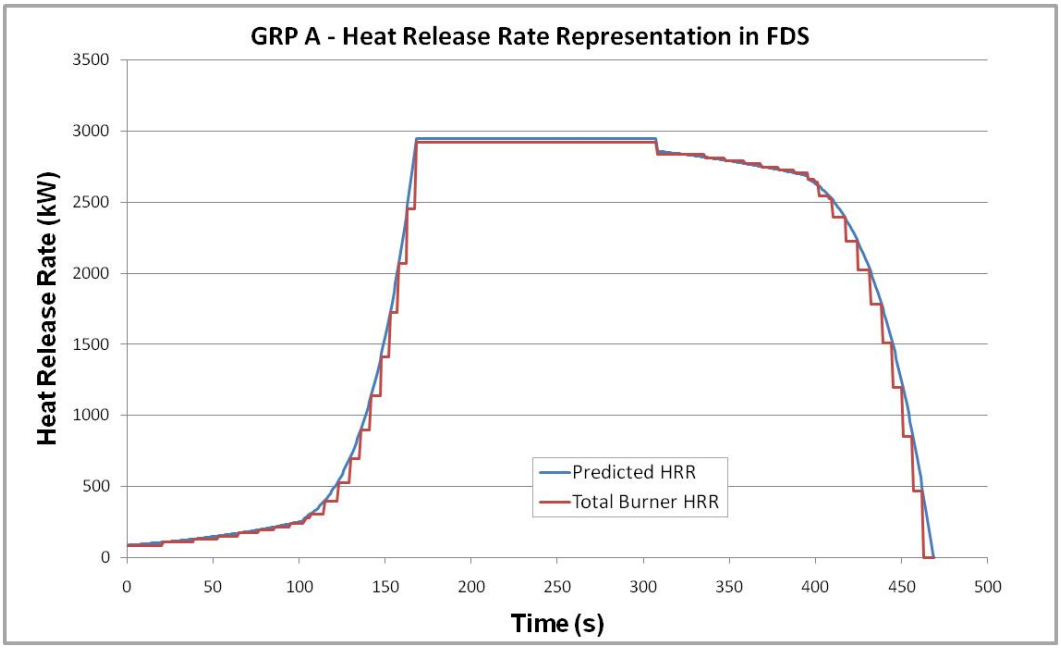

Figure 39. GRP A – Heat Release Rate Curve Representation in FDS

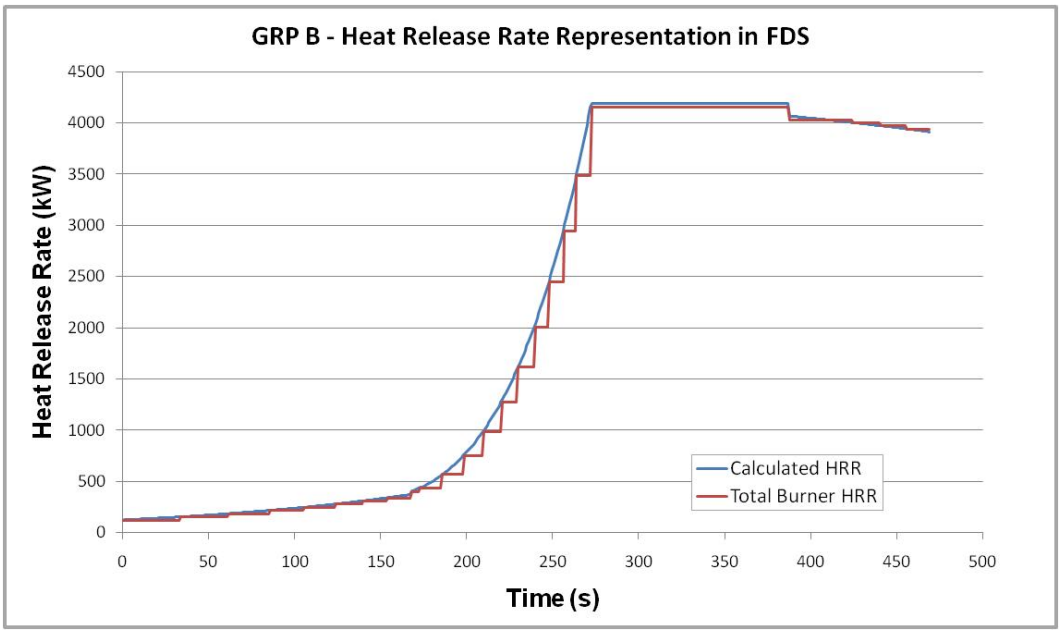

Figure 40. GRP A – Heat Release Rate Curve Representation in FDS

7.5 CFD Analysis Results

The image below provides a snapshot of flame spread during one of the simulations. Flashover conditions were eventually observed in the vehicle given both types of GRP material.

Figure 41. Example FDS Output Showing Predicted Flame Spread

Figure 42 provides a comparison of the total heat release rate of the passenger rail vehicle given the two types of lining materials being considered.

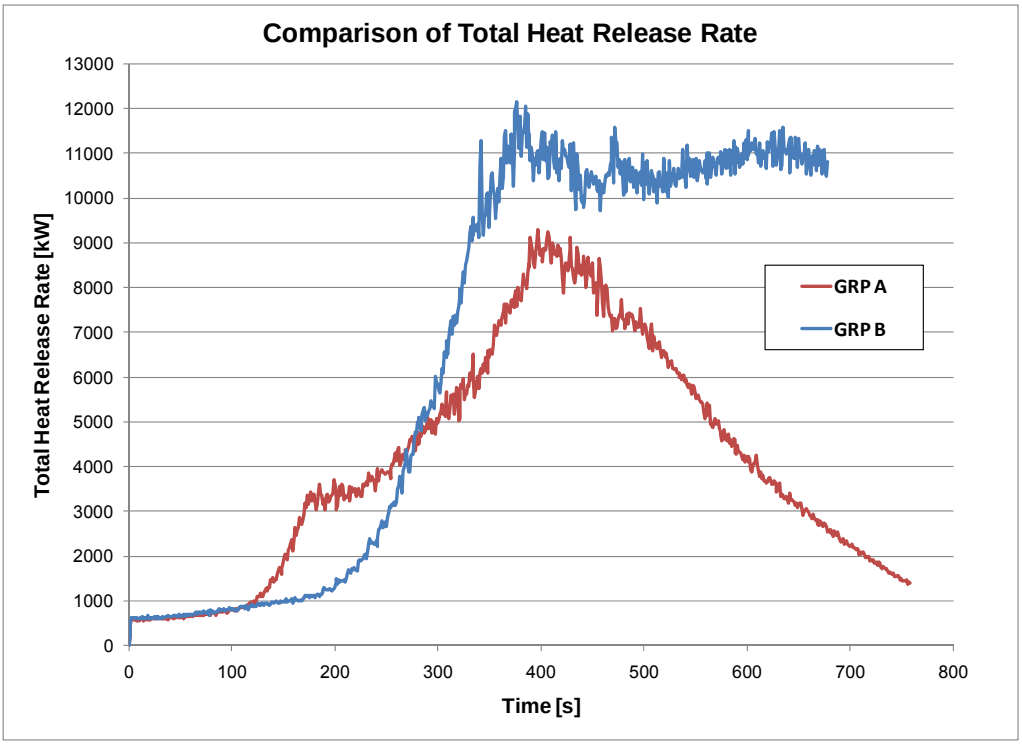

Figure 42. Comparison of Total Heat Release Rates from FDS

The GRP A material results in a peak heat release rate of approximately 9.2 MW and exhibits a defined decay phase shortly after the peak heat release rate is experienced. The model incorporating GRP B calculated a maximum heat release rate of approximately 12.0 MW with a sustained heat release rate of approximately 11.0 MW subsequent to the peak. Because the maximum heat release rate was the focus of this analysis, the simulations were not run until complete burn-out.

7.6 Conclusions of Analysis

The example analysis provided here has verified that the installation of the material designated GRP A will result in a maximum heat release rate of less than the stated criteria of 11.0 MW given a typical passenger vehicle design. The other material considered, GRP B, results in a maximum heat release rate of approximately 12 MW.0, which exceeds the stated limit.

This analysis has not specifically addressed life safety within the rail vehicle or associated tunnels or stations, nor has it considered the possible impact of additional design initiating fires, vehicle layouts, or ventilation conditions. Each of these factors may need to be considered when carrying out this type of study.

This analysis is included here as an example of the use of the proposed methodology and does not represent any actual rail system, rail vehicle, or material.

8 Limitations, Applications and Future Research

8.1 Limitations

This approach uses a combination of small-scale test data, simplified analysis tools (b-parameter, simple flame spread model), and complex computational fluid dynamics modeling (using the tool Fire Dynamics Simulator, FDS). Each component has associated uncertainty.

At the small-scale test level, differences in materials (from one sample to another), in data collection from different test apparatus, and potential errors in reporting may exist. Development of a common test protocol, apparatus calibration protocol, and data reporting protocol would help reduce uncertainty in the data.

Because the simplified analysis level (b-parameter, flame spread model) is intended to provide a simple screening approach, some of the complexity associated with factors such as geometry of vehicle configuration was ignored (e.g., it was assumed that walls and ceilings were flat with no obstructions or curvature). Sensitivity analysis could be undertaken to better understand the importance of these issues to the level of accuracy needed in the screening approach, and modifications could be made if appropriate.

With respect to computational modeling, small-scale tests of individual materials cannot generally be used to directly predict large-scale fire behavior within a rail vehicle because tests of individual materials do not consider the interplay between adjacent materials and the geometry of the fire compartment, as well as ventilation and other environmental conditions. In order to draw more useful conclusions regarding vehicle fire hazards using small-scale test data, additional computational analyses are required. This would include obtaining additional small-scale test data on a wider range of materials, considering a broader range of initiation fires, and modeling a more extensive set of vehicle geometries and ventilation conditions.

8.2 Potential Applications

The methodology outlined in this report has several potential applications, including the following:

Fire hazard assessment of existing stock: Whereas it is costly to burn complete vehicles to understand fire development issues, this approach allows for small samples of materials to be tested (from an existing vehicle, or from parts for a vehicle), and analysis to be conducted to obtain an indication as to what size initiation fire might lead to full vehicle involvement, and what the resultant fire size would be. This could be used as part of a threat, vulnerability and risk assessment (TVRA) of vehicles to understand impacts on passengers and other vehicles.

Fire hazard assessment of critical infrastructure: As noted above, this methodology can be applied to help better understand the resultant fire size from a fully-involved vehicle. This could be used as part of a threat, vulnerability and risk assessment (TVRA) stations, tunnels and other rail infrastructure to assess impact from the vehicle fire. This could range from smoke control in a station to thermal impact on tunnel lining or bridge decking. This could be applied to existing infrastructure or to new designs. With a current focus on high-speed rail, for example, such an approach may be beneficial for assessing a wide range of potential fire scenarios – accidental or deliberate – and to support assessment of mitigation options.

Options analysis for new vehicle design: At the vehicle design stage, the methodology can be applied to help assess the performance of different interior lining materials with

respect to resistance to initiation fires of concern and contribution to overall fire size. Manufacturers can use this information to make informed judgments about material use in vehicles. With a current focus on high-speed rail, for example, such an approach may be beneficial for assessing a wide range of vehicle options.

Regulatory support: Current regulations generally require testing of material flame spread at a single heat flux level (e.g., see the 2008 report prepared for the FTA [6]). As demonstrated by this research; however, a material may perform differently at different heat flux levels, such as resisting ignition and self-propagating flame spread to lower levels, to igniting and self-propagating flame at higher heat flux levels. Based on the level of risk or hazard deemed tolerable from a regulatory perspective, this methodology could be used as support for modifying flame spread test requirements, such as perhaps requiring a range of incident heat fluxes and reporting outcomes. With a current focus on high-speed rail, for example, it may be anticipated that new materials will be suggested, and new or more robust testing may be desired to understand how material perform as part of regulatory benchmarking.

8.3 Future Research

As outlined above, additional research at all stages of material testing, screening tool development, and computational analysis would be helpful to better understand and address uncertainty and variability. If deemed necessary, refinements in the screening approach and modeling approach could be made to help produce better results.

More extensive computational modeling, over a broader range of materials, vehicle configurations, and ventilation conditions would be helpful in identifying and addressing uncertainty in the computational modeling and from refining the efficacy of the methodology for the potential applications outlined above.

Tools for threat, vulnerability and risk assessment (TVRA) and regulatory analysis and policy setting could be developed based on the methodology. Options might range from providing a more formalized structure for the basic concepts outlined herein, to development of more risk-informed performance-based analysis techniques for fire hazard analysis, to development of risk-cost optimization approaches or models for setting regulatory targets.

9 Summary and Conclusions

Whether a small fire in a passenger rail vehicle stays small or grows to encompass the vehicle, and how large the ultimate fire may become, is largely a function of the initiation fire, vehicle interior materials (interior lining / components and contents), vehicle configuration and ventilation. Assuming fixed configuration and limited ventilation options, significant variables become the initiation fire, interior materials and contents.

Evaluation of the relative fire hazards represented by different interior lining materials as exposed to various initiation fire scenarios can be costly and time-consuming if full-scale fire tests are utilized. However, small-scale fire tests, such as those that utilize the cone calorimeter apparatus, are less expensive (by far) and numerous tests can be carried out in a given day. Small-scale test data, coupled with initiation fire data and computational modeling, can be used to cost-effectively assess a wide range of scenarios and material combinations for existing and proposed vehicle designs.

Although computational modeling has been used for some time, previous generation tools lacked the sophistication to address several important features, including flame spread and contribution of interior lining materials.

This report has proposed a methodology for determine flame spread and fire growth behaviors within rail vehicles based upon small-scale fire tests. Through the application of a relatively-simple screening tool capable of identifying a material's propensity to spread flames, a spreadsheet-based initial flame spread prediction methodology, and computational fluid dynamics fire modeling tools, prediction of the overall fire hazard represented by a given vehicle configuration is possible.

The proposed methodology has been demonstrated through a hypothetical scenario in which two possible lining materials were compared. The approach demonstrated that one of these materials was not appropriate given the stated stakeholder goals, while a second material represented an acceptable level of fire hazard. This analysis was not intended to represent a specific vehicle or rail system, but rather was used to demonstrate how the proposed methodology could be applied.

10 Nomenclature

10.1 Variables

Variable	Definition
A	Area (m²)
b	b-parameter (flame spread parameter)
c	Specific heat (kJ/kg/K)
CHF	Critical heat flux (kW/m²)
D	0.08H (representative t-shape depth) (m)
D	Diameter of the fire
E	Total energy release rate (kW)
$\dot{E}$	Average energy release rate (kW)
F	View factor
H	Ceiling height (m)
k	Thermal conductivity (W/m/K)
k	Flame length before pyrolysis (m)
q	Heat flux (kW/m²)
Q	Heat release rate (kW)
ρ	Density (kg/m³)
t	Time (s)
T	Temperature (C)
V	Velocity (m/s)
W	Ceiling width (m)
x	Length (m)
X	Fraction
Z_f	50^{th} percentile flame height (m)

10.2 Subscripts

Subscript	Definition
b	Burnout zone
b0	Burning duration
bs	Source burnout
c	Char
e	External
end	End of measured time
f	Flame zone
fl	Flame
ig	Ignition
p	Pyrolysis zone
p0	Pyrolysis variable at source ignition time
p1	Pyrolysis variable at burnout time
p0h	Height of initial source fire
p0w	Width of initial source fire
R	Radiative

10.3 Superscripts

Superscript	Definition
“	Per unit area (m^{-2})
s	Source

11 References

[1] NFPA 130, Standard for Fixed Guideway Transit and Passenger Rail Systems, 2010 edition.

[2] Chicago Rapid Transit. www.chicago-l.org

[3] www.nycsubway.org

[4] Kawasaki Heavy Industries. http://www.khi.co.jp/products/rolling_stock/

[5] Kawasaki Heavy Industries. www.kawaskirailcar.com

[6] National Association of State Fire Marshals (NASFM). *Recommended Fire Safety Practices for Rail Transit Materials Selection*. Prepared for the U.S. Department of Transportation, Federal Transit Administration, Office of Safety and Security,. 2008.

[7] Kirk, D. "Use of Dangerous Materials Cited in Korean Subway Fire." *The New York Times*, p. 4. February 21, 2003.

[8] Babrauskas, V. "Heat Release Rates," in *SFPE Handbook of Fire Protection Engineering, Fourth Edition. Section 3, Chapter 1.* Quincy, MA: National Fire Protection Association, 2008.

[9] American Society for Testing and Materials (ASTM). Standard Test Method for Heat and Visible Smoke Release Rates for Materials and Products Using and Oxygen Consumption Calorimeter. ASTM E-1354. Annual Book of ASTM Standards. Volume 07.07, 1997.

[10] ISO 5660-2, Reaction to Fire Tests - Heat Release, Smoke Production, and Mass Loss Rate Standard, 2002.

[11] Huggett, C., "Estimation of the Rate of Heat Release by Means of Oxygen Consumption," Fire and Materials 12: 61-65, 1980.

[12] Babrauskas, V., "The Cone Calorimeter," in *SFPE Handbook of Fire Protection Engineering*, Second Edition, Ed. DiNenno P, 3-37 to 3-52, National Fire Protection Association, Quincy, MA, 1995.

[13] Janssens, M., "Calorimetry," in *SFPE Handbook of Fire Protection Engineering*, Second Edition, Ed. DiNenno P, 3-16 to 3-36, National Fire Protection Association, Quincy, MA, 1995.

[14] McGrattan, K. et. al., "Fire Dynamics Simulator (Version 5) Technical Reference Guide – Volume 3: Validation," NIST Special Publication 1018-5. 2008.

[15] Rehm, R. and Baum, H, "The Equations of Motion for Thermally Driven, Buoyant Flows," Journal of Research of the NBS 83: 297-308, 1978.

[16] Quintiere, J.G, "Simplified Theory for Generalizing Results from a Radiant Panel Rate of Flame Spread Apparatus," *Fire and Materials* **5**: 52-60 (1981).

[17] Cordova, J.L., Walther, D.C., Torero, J.L., and Fernandez-Pello, A.C. "Oxidizer Flow Effects on the Flammability of Solid Combustibles," *Combustion Science and Technology* 164: 253-278 (2001).

[18] Lautenberger, C., Rein, G., and Fernandez-Pello, A.C., "The Application of a Genetic Algorithm to Estimate Material Properties for Fire Modeling from Bench-Scale Fire Test Data." *Fire Safety Journal*, 41: 204-214. 2006.

[19] Rein, G., Lautenberger, C., Fernandez-Pello, A.C., Torero, J.L., and Urban, D.L., "Application of Genetic Algorithms and Thermogravimetry to Determine the Kinetics of Polyurethane Foam in Smoldering Combustion." *Combustion and Flame,* 146: 95-108. 2006.

[20] Cleary, T., & Quintiere, J. "A Framework for Utilizing Fire Property Tests." *Third International Symposium on Fire Safety Science*, 647-656. 1991.

[21] Cleary, T., & Quintiere, J. *A Framework for Utilizing Fire Property Tests*. Gaithersburg, Maryland: National Institute of Standards and Technology. 1991.

[22] Avila, M. B. *The Effect of Resion Type and Glass Content on the Fire Engineering Properties of Typical FRP Composites*. Worcester, MA: Worcester Polytechnic Institute, 2007.

[23] Mowrer, F. W., & Williamson, R. B. "Flame Spread Evaluation for Thin Interior Finish Materials." *Fire Safety Science - Proceedings of the Third International Symposium* (pp. 689-698). England: Elsevier Science Publishers LTD, 1991.

[24] Quintiere, J., Harkleroad, M., & and Hasemi, Y. "Wall Flames and Implications for Upward Flame Spread." *Combustion Science and Technology*, Vol. 48 , 191-222. 1986.

[25] Saito, K., Quintiere, J., & and Williams, F. "Upward Turbulent Flame Spread." *Fire Safety Science - Proceedings of the First International Symposium*, 75-86. 1986.

[26] Quintiere, J. G. "A Simulation Model for Fire Growth on Materials Subject to a Room-Corner Test." *Fire Safety Journal,* 20 , 313-339. 1993.

[27] Mitler, H. and Rockett, J., "Users Guide to FIRST, a Comprehensive Single-room Fire Model," NBSIR 87-3595, National Bureau of Standards, Gaithersburg, MD, 1987.

[28] Jones, W., Forney, G., Peacock, R., and Reneke, P., "A Technical Reference for CFAST: An Engineering Tool for Estimating Fire and Smoke Transport," NIST TN 1431, National Institute of Standards and Technology, Gaithersburg, MD, 2003.

[29] McGrattan, K. et. al., "Fire Dynamics Simulator (Version 5) Technical Reference Guide – Volume 1: Mathematical Model," NIST Special Publication 1018-5. 2008.

[30] McGrattan, K, Klein, B., Floyd, J., Hostikka, S., "Fire Dynamics Simulator (Version 5) – User's Guide," National Institute of Standards and Technology, NIST Special Publication 1019-5, 2008.

[31] Brehob, E., Kim, C., and Kulkarni, A., "Numerical Model of Upward Flame Spread on Practical Wall Materials," Fire Safety Journal 36: 225-240, 2001.

[32] Quintiere, J., "A Simulation Model for Fire Growth on Materials Subject to a Room-Corner Test," Fire Safety Journal 20: 313-339, 1993.

[33] Sorathia, U., Long, G., Gracik, T., Blum, M., and Ness, J., "Screening Tests for Fire Safety of Composites for Marine Applications," Fire and Materials 25: 215-222, 2001.

[34] Lautenberger, C., Wong, W., Coles, A., Dembsey, N., Fernandez-Pello, C., "Large-scale Turbulent Flame Spread Modeling with FDS5 on Charring and Noncharring Materials" *Fire and Materials* (2009).

Appendix A

Review of Past Passenger Rail Fire Incidents

A1 Past Passenger Rail Fire Incidents

Month	Country	Vehicle Configuration	Ignition Source	Fire Location	Consequences	Miscellaneous
August 2009	Canada	Passenger Train	Locomotive caught fire.	Loco-motive	More than 300 passengers had to walk along the tracks to the nearest road to board buses to finish their journey. At least 13 required treatment for bug bites, allergic reactions and some minor bumps and bruises.	
July 2009	Italy	Freight Train	Police said that five wagons at the back of the fourteen-wagon train, which was on its way to Pisa, left the tracks and crashed next to the station. The crash ruptured the tanks carrying the LPG and the fumes ignited.	Entire Train	At least sixteen people including three children were killed and thirty-four were injured	
January 2009	UK	Freight Train	A freight train laden with fuel derailed and burst into flames as it crossed a bridge. Six of the ten wagons were derailed and one caught fire. The train had been carrying heating oil and diesel from Grangemouth refinery to a terminal in Kilmarnock.		No injuries were reported	Flames shot 50ft into the air and a plume of black smoke drifted above the scene
June 2009	U.S.A.	Amtrak Locomotive	The second one - a 40-year-old engine - shot sparks high into the air from its exhaust stack. It was like they were falling out of the engine. It looked like a giant sparkler," said Jacqueline Scharff, who watched from her backyard patio as the train passed slowly. The cause of sparks from the locomotive was apparently carbon buildup in the diesel engine.	Brush along side of track.	One house was seriously damaged and other homeowners lost fences and trees to the rapidly spreading flames. "We've had other fires before . . . and I'm certainly concerned. Once one house starts to burn, it's only a matter of time before others can catch fire, too."	A series of Main Line fires - including a serious house blaze - caused by a malfunctioning Amtrak
Nov 2009	U.S.A.	Regional Commuter Train	A SEPTA official said the likely cause was electrical. Other news reports say it might have been the heater or the traction motor.	Train's First Car	The train was packed with nearly 700 passengers. Nobody was injured, but the suburban commuter line was shut down for two hours, complicating an already chaotic rush hour.	This incident happened the day after a large strike in this transit system. The incidents are thought not to be related. This train has been in service since 1965.
April 2009	UK	Commuter Train	Unknown	Under-carriage	Delays	Passenger Simon Boynton said: "There were flames under the train and smoke. The fire was put out quickly though."

Month	Country	Vehicle Configuration	Ignition Source	Fire Location	Consequences	Miscellaneous
Sept 2009	U.S.A.	Passenger Train	Overload or short circuit sparked.	Tunnel Fire	No one was hurt, but subway service was suspended at the end of rush hour in the middle of the city, causing confused crowds to form around several stations around the city.	Last night's incident was the third in three days for the T. On Tuesday, a train from Worcester hit a metal back stop and came to an abrupt stop at South Station, injuring 18 people. Monday night, two trains nearly collided on the Worcester line.
May 2009	China	Passenger Train	We are investigating the cause of the fire, a fire brigade lieutenant said. One likely cause is an electric short circuit in the air conditioning system aboard the train.	Inside of Train	Fortunately, the spokesman said, the train was empty. There were no casualties. Fire engines were dispatched by the Chiayi fire brigade to douse the fire in half an hour.	The system has not been inspected for quite some time, the Hungtu spokesman said. Checkups on the air-conditioning system is the third echelon inspection, which take place every three years, he added.
Nov 2009	U.S.A.	Commuter Train	The fire is believed to be caused by an electrical short either from the heater or the traction motor.	Inside Train	No one was injured in the fire. More than 100 people needed to be evacuated from the commuter train even further complicating the morning rush.	This was a day after the mass transit workers went on strike.
August 2008	India	Passenger Train	Short circuit in the train's wiring. The Commissioner of Railway Safety in its provisional findings said that the incident had occurred due to some highly inflammable substance kept in the sleeper coach by unidentified persons in the S-10 coach of Secunderabad-Kakinada Goutami Express.	Inside Train	AT least 32 people died and 9 injuries when several coaches of a train caught fire in southern India.	The tragedy struck when the passengers were fast asleep making it impossible for many of them to escape from the blaze.
Sept 2008	U.S.A.	High-Speed Line	Sparks from a component on the electrified third rail ignited rail ties along the westbound tracks at 3:05 p.m., causing PATCO operators to turn off the power that propels the trains, spokesman Ed Kasuba said.	Track Fire	Forced a six-car train to stop on the Ben Franklin Bridge, stranding 51 passengers for several hours, authorities said. No one was injured, although a pregnant woman and an asthmatic man were taken to Pennsylvania Hospital as a precaution	"There was never any smoke in the train," Kasuba said. "The car was never on fire. The sparks were on the track." He said the train was stopped "as a precaution."
August 2008	UK	High-Speed Train	Fire initially started in the exhaust system.	Exhaust System	No one was injured by the fire, but there was significant delays and cancellations to services because of the major holdup.	

Month	Country	Vehicle Configuration	Ignition Source	Fire Location	Consequences	Miscellaneous
January 2008	South Africa	Train Engines and Carriages	Vandals who burnt six train engines and 18 carriages north of Pretoria, Friday. Exact ignition locations and materials are unknown.	Train Engine and Loco-motive; Exact location is unknown	Commuters were kept waiting for two hours as a result of train delays due to a power failure caused by storms. The angry commuters caused damage estimated at about R150 million to the trains and R2.5 million would be needed to restore damaged lines. According to Metrorail, it will take three to six months to restore train services at the affected train stations.	During 2006/07, the SARCC/ Metrorail reported in excess of 800 incidents of vandalism, including theft, wilful damage of operational assets and acts of sabotage in their environment. These incidents cost the operator in excess of R50 million.
April 2007	U.S.A.	Rail car	Overheated motor.	Train Engine	As many as 100 firefighters responded to the blaze, extinguishing it quickly and evacuating 30 to 70 riders on board at the time. No injuries were reported.	"This is very rare to have a fire on a train," she said. "It's really very unusual, but we will investigate to see what happened."In January, three fires within a week on the tracks at Farragut North shut that station repeatedly during the weekday morning commute. Metro officials concluded that two of those incidents were caused by stray electrical currents, and the third was the result of friction igniting paper that had been thrown onto the tracks.
January 2007	U.S.A.	Rail car	Short circuit caused smoke to come out of bolts that support the electrified rail	Electrical Rail	Significant delays as Metro shut off power to that stretch of track, and 76 District fire and emergency personnel responded	
May 2007	U.S.A.	Passenger Train	A lighted cigarette was believed to have sparked a fire under the Longfellow Bridge	Chain-link-enclosed crawl-space that spans the width of the bridge.	Forced the closure of the road and the Charles/MGH MBTA Station and triggered traffic backups on major surrounding arteries, including Storrow Drive, authorities and commuters said. MBTA officials said a total of 425 people were evacuated from trains that were on or near the bridge at the time of the fire. Bridge and train traffic was shut down for more than two hours while the fire was doused and the bridge was in-spected.	"You couldn't see the station," MacDonald said. "There was thick black smoke everywhere."
Feb 2007	India	Passenger Train	Two suitcases packed with unexploded crude bombs and bottles of petrol were found in carriages not hit in the attack, and it is believed the fire was set off by an identical device. Home-made bombs were not powerful and were simply intended to start a fire on the train.		At least 66 people were killed. At least 30 passengers who were injured in the inferno.	India's junior home minister, Sriprakash Jaiswal, said the home-made bombs were not powerful and were simply intended to start a fire on the train one day before Pakistani Foreign Minister Khursheed Kasuri was to arrive in New Delhi for talks on the ongoing peace process.

Month	Country	Vehicle Configuration	Ignition Source	Fire Location	Consequences	Miscellaneous
April 2007	UK	Passenger Train	As the train pulled into the station one of the youths set fire to the paper that were stacked on the seats. The fire set the train seat alight and caused the carriage to fill with smoke.	Inside Train	Delays but no injuries.	
August 2006	U.S.A.	Subway Trains	Fire marshals determined that the fire was accidental. Investigators found rubbish and cigarette butts around the source of the fire and suspected that homeless people might have spent time at the site, he said.	Track Fire	At least 25 people received minor injuries, including 10 passengers and three firefighters who were treated at hospitals for smoke inhalation, the authorities said. Subway and car traffic between Brooklyn and Manhattan was snarled for hours.	Three of the B train's 10 cars were in the smoke-filled tunnel, and the rest were on the bridge. An eight-car D train, behind the B train on the bridge, also stopped. The passengers said they tried to stay calm, but were confused by a lack of instructions.
August 2006	U.S.A.	High-Speed Line	A portion of a restraining chain that had been left under one car after weekend maintenance touched the third-rail power source, causing an electrical arc that created flames and smoke, the commuter railroad said.	Under-carriage	Sent nearly 30 people to hospitals. Service was halted for more than 21/2 hours.	
August 2006	China	Passenger Train	A preliminary investigation has excluded the possibility of foul play, but the cause of the fire has not yet been released. Further investigation is under way, according to the statement.		No deaths or injuries were reported.	According to the statement, the fire did not affect the operation of the other maglev line and it was brought under control one hour later.
April 2005	U.S.A.	Subway	Arcs of electricity from a substation that converts alternating current.	Under-ground Room	The blaze, inside a tunnel, injured five riders and one transit worker and forced the evacuation of more than 600 people from three subway trains. One worker, a power maintenance assistant, was briefly hospitalized for minor burns. Three riders -- one of them a pregnant woman and another a deaf woman who has asthma -- were hospitalized for minor injuries. Two other riders were treated at the scene for smoke inhalation.	The flames sent thick gray smoke through the tunnels and up into the air around the station. Service on the A, B, C and D lines was suspended or rerouted for more than three hours.
Oct 2005	U.S.A.	Subway Lines	The cause of the fire was not known.	Storage Room	Seven subway lines were crippled at the height of the morning rush yesterday by an electrical fire at the West Fourth Street station, leading to long delays for an estimated 125,000 commuters	
Jan 2005	U.S.A.	Subway Lines	Homeless person trying to keep warm.	Transit Control Room	Worst damage to subway infrastructure since the terrorist attack of Sept. 11, 2001	

Month	Country	Vehicle Configuration	Ignition Source	Fire Location	Consequences	Miscellaneous
Jan 2005	South Korea	Commuter Subway Train	Arsonist set blaze with rolls of newspapers after pouring volatile liquid at Cholsan Station.	Inside Train	Gutting three train cars and inflicting minor burns on one woman with no other casualties. However, as the empty subway train was heading to its final station at 7:25, the fire, which was believed to be extinguished, started up again and burned the last three rail cars of the train.	Passengers evacuated immediately while subway station officials put out the fire with fire extinguishers.
Jan 2004	China	Passenger Train	Fire to a bottle of inflammable liquid and attempted to ignite 5 bottles of suspected thinners and 5 canisters of liquid petroleum gas (LPG) he had brought in by a handcart.	Inside Train	14 people were injured. The MTR spokeswoman said a total of 5,000 passengers had been affected mainly by the temporary suspension of train services on the Tsuen Wan Line. She said about 1,200 passengers inside the train and the station at the time of the fire were evacuated.	MTR By-law Clause 39 prohibits people from carrying inflammable and dangerous goods into MTR premises. Gaffney said MTR trains were built with fire-resistant material, with the controller's room door capable of with-standing fire for 30 minutes. As to why the train continued to the Admiralty station before passengers were evacuated, Gaffney said it was easier to remove passengers at the platforms rather than inside tunnels.
Sept 2004	U.S.A.	Multiple trains affected by tunnel fire.	Transformer fire. Surge apparently sparked some type of fire inside the tunnel.	Tunnel Fire	Halted train traffic for hours yesterday and briefly shut down the terminal, causing confusion and long delays for more than 100,000 riders trying to get home for the evening.	The fire caused heavy smoke in the tunnel, said Tim Hinchey, a Fire Department spokesman. Firefighters trying to get at the blaze were slowed by limited visibility as they gingerly descended a narrow spiral staircase to the tunnel floor, he said.
Sept 2004	U.S.A.	Multiple trains affected by tunnel fire.	Falling cable causes power surge.	Tunnel Fire	That mishap on Monday afternoon, railroad officials said, set in motion the chain of events that brought the station to a standstill and disrupted the trip home for more than 100,000 commuters.	The smoke was caused by the burned insulation around the wires.
July 2003	U.S.A.	Subway	Shoe became dislodged and caused a short circuit.	Over-carriage	100 people were treated for smoke inhalation. The smoke was so heavy that almost everyone on the train and in the station, at York Street near the Manhattan Bridge, required treatment at the scene, and more than 60 people were taken to hospitals, officials said. Train service at the station, which serves only the F line, was redirected for much of the day.	

Month	Country	Vehicle Configuration	Ignition Source	Fire Location	Consequences	Miscellaneous
Nov 2003	U.S.A.	Passenger Train	Cable for the electrified third rail.	Track Fire	An electrical fire on a subway track in Harlem sent smoke billowing through the tunnels yesterday morning and forced the evacuation of a train full of passengers, stalling morning commuting for thousands.	
Feb 2003	South Korea	Subway	Man ignited a container of paint thinner with a cigarette lighter.	Inside a Subway Train	Took the lives of more than 130 people on two subway trains.	Spread quickly, reaching approximately 2,000 degrees in heat. The heat was so intense that it rapidly carried flames from the first train to the second, and down the cars of each train, twisting aluminum, turning strap handles and floor covering to wax and burning bodies so totally that identifica-tion of most will never be possible. Most of the deaths and injuries were caused by inhalation of toxic fumes from the vinyl and plastic seat cushions. Investigators also described faulty emergency signals, poor communications and misjudgment on the part of sub-way workers with little or no training in how to cope with crisis. The cars apparently did not have fire extinguishers. Although emergency lights did go on, sprinkler systems and ventilation systems failed, apparently because they were not linked to a backup power system.
May 2003	UK	Passenger Train	Flames broke out in the engine compartment.	Engine Compart-ment	Damaged engine compartment. Enterprise manager Ken McKnight said travelers were not in much danger as the fire was in the engine room.	He added: "We sat for about 30 minutes before we were finally evacuated.
March 2003	UK	Voyager Train	An investigation has been launched to find out the cause of the fire, which started in the lagging around the exhaust pipe on the outside of the end of the carriage.	Exhaust Pipe	Minor delays.	Virgin insisted there had been no danger of the train's diesel fuel tanks being ignited.

Month	Country	Vehicle Configuration	Ignition Source	Fire Location	Consequences	Miscellaneous
March 2003	UK	Voyager Train	Both were in the train's exhaust system	Exhaust Pipe	Fire forced passengers to be evacuated. No one was injured.	AN investigation was under way last night after a fire forced passengers to be evacuated from one of Virgin's (pounds) 400m fleet of new trains for the second time in a fortnight. The fires are the first to affect Virgin's fleet of Bombardier-built trains, called Voyagers, since they were introduced to its Anglo-Scottish cross-country franchise in May 2001.
April 2003	UK	Diesel Passenger Train	Vandals had thrown things over the electric overhead wires.	Over-carriage	15 passengers were shepherded to safety. 'Luckily none of the passengers were hurt and moved to the back of the train to safety as soon as the fire started.	'Throwing things over electric cables is so dangerous and this incident could have been much worse. Fortunately this sort of thing is very rare.'
Nov 2002	France	Express Train	The fire appeared to have started in an electrical control panel in a first-class sleeper car.	First Sleeping Car	At least 12 people, including 5 members of a family vacationing from Connecticut became engulfed.	"Preliminary investigations indicate that, given the relatively small number of burns on the bodies, except for two who suffered burns on their extremities, the deaths were caused by asphyxiation." Deutsche Bahn said its sleeping cars are fitted with fire extinguishers, but usually not with smoke detectors because in many trains smoking is still permitted in some sections.
Feb 2002	Egypt	Rail Passenger Train	The fire is thought to have been ignited by the explosion of a small stove used to make tea or heat food.	Inside a Passenger Car	More than 370 passengers were killed, some of whom leapt to their deaths on the tracks in an effort to escape the flames. It consumed seven cars before train engineers realized what was happening and uncoupled the flaming cars from the front nine	Mr. Sherif said the train had emergency brakes and some fire extinguishers but it is likely that the passengers were unable to find them in their panic. Some passengers disputed that, saying their cars lacked emergency brakes.Official government statistics indicate that nearly 5,000 people died in railroad related accidents in both 1998 and 1999, the most recent years for which figures are available, but those numbers include incidents like collisions at rail-road crossings.
Dec 2002	UK	Passenger Train	ARSONISTS piled up seat cushions on a train and set them on fire.	Inside Train	Fire crews tackled the blaze but the carriage was destroyed and damage estimated at about pounds 250,000.	
April 2002	Australia	Train Carriage	Exact ignition source is unknow, but the last carriage was intentionally ignited by an arsonists.	Last Carriage	$1.5 million blaze, which gutted a carriage and endangered the lives of a dozen passengers.	"It is fortunate that it has occurred when the train was stationary at a station. There was clear potential there for a worse occurrence."

Month	Country	Vehicle Configuration	Ignition Source	Fire Location	Consequences	Miscellaneous
Jan 2002	UK	Commuter Train	A spokesman said the fire was caused by an electrical component underneath the train but investigations were still under way.	Under-neath the Central Cabin	Railtrack said 16 trains were delayed for 127 minutes, a further four diverted and two cancelled as a result of the incident.	"The train was a 1960 vintage rolling stock which should have been replaced by now." The latest blaze follows two fires last year involving commuter trains at a neighboring station.
Jan 2002	UK	High-Speed Line	Flames leapt from one of the power cars just after the high speed train had taken on more passengers. The flames were spotted coming from the exhaust of one of the trains power cars as it stood at platform two.	Exhaust Pipe	No one was hurt.	"It was a fire in the traction unit of the train. It was removed very, very quickly.
March 2002	Indonesia	Passenger Train	Electrical short circuit in the cafeteria carriage.	Train's Cafeteria Carriage.	No casualties were reported. Hundreds of passengers, including a journalist with The Jakarta Post, were forced to jump out of the ill-fated train and were later transported to Surabaya by an Argo Bromo executive train.	Crew members were powerless to put out the blaze which razed both carriages as fire-fighting equipment failed to work properly. Many passengers blasted the poor effort by the train's crew to put out the blaze following the malfunction of the fire extinguishers.
May 2002	UK	Passenger Train	The fire broke out in the central carriage of the three-carriage train. Exact ignition source is unknown.	Inside of Train	Two men, including one member of rail staff, were taken to Monklands District General hospital where they were treated for smoke inhalation. A woman who suffered minor injuries was treated at the scene.	
June 2000	U.S.A.	Passenger Train	Yesterday's fire was caused by plastic brushing up against the 750-volt "third rail" that provides electricity to the trains.	Track Fire	No one was injured, but all trains were stopped causing delays.	The new policy, Capt. Resnick said, was fully implemented as planned, with Metro evacuating the underground area, calling the fire department and making sure the fire was contained.
June 2000	U.S.A.	Subway	Loose door frame in a subway tunnel that shook free from the concrete wall and fell onto the track bed moments before a District-bound train ran over it and caught fire.	Track Fire beneath subway	The Green Line fire, in which no one was seriously hurt, marked the seventh time in two weeks that Metro stations were closed because of a report of fire or smoke.	Metro has also been struggling with the ways it responds to crises. Officials acknowledged the system fumbled a serious April 20 fire, in which Metro's operations control center knowingly sent a train filled with 273 passengers toward a tunnel fire.
May 2000	U.S.A.	Metro Station	Sparked when ballast lights on the track bed overheated	Track Fire	No one was injured by the flames	Transit officials called the D.C. fire department immediately. The only problem was, Metro sent the firefighters to the wrong station--Archives-Navy Memorial, three stations south of the trouble spot.

Month	Country	Vehicle Configuration	Ignition Source	Fire Location	Consequences	Miscellaneous
Sept 2000	U.S.A.	Metro Train	Batteries and wires in the undercarriage.	Under-carriage	About 35,000 commuters on the line, Metro-North's busiest, were delayed by an hour or more. There were no serious injuries, but a conductor was taken to the hospital for smoke inhalation and a passenger was treated for stress.	The train was partly in the station, but the back end, where the fire was, was in an underpass tunnel, which quickly filled with smoke from burning insulation and electrical housing, Chief Kiernan said.
August 2000	U.S.A.	Subway Lines	600-volt power cable	Cables beneath the street	Forced the closing of four of the city's busiest subway lines yesterday just as the evening commute was beginning, stranding tens of thousands of riders in Manhattan and Brooklyn	
Feb 2000	Australia	Passenger Train	It is believed the fire began when a fuse caught a light on the pentograph, a device which conducts electricity from the cables to the train. Fire may have been caused by dust accumulating through the vents.	Vents of the Rear Carriage	The train was stopped for almost one hour and all west-bound services were delayed before it was moved to a siding at Valley Heights.	"This is the first one I have dealt with in 16 years, normally the fires we have, people start inside the carriages," Four carriages of the 6.17am Sydney to Mount Victoria intercity service were cleared after SRA staff noticed smoke above the train's roof as it pulled into the station. Mr. Taylor said.
May 2000	U.S.A.	Freight Train	exhaust of a freight train.The sparks started as many as 10 fires as the train.	Track/ Wood Fire	Charred 115 acres in Pine Hill and 15 acres in Winslow Township.	Hasselhan said that when the train began climbing a slight grade, it caused the engine to ignite a carbon buildup.
Nov 2000	Australia	Cable Car	The cause of the blaze, which is believed to have started in the rear of the train, is unknown,	Rear of Train	At least 159 skiers and snowboarders killed. "The force of the fire was so great that the surroundings melted," said Maj. Lang, one of the investigators. Many bodies - some of them twisted together - were discovered about 300 yards from the train, indicating that the victims died from smoke and chemical poisoning after escaping the train.	"Because there was such intense heat in the tunnel, the features usually used to identify someone - eyes, lips, nose - are no longer there," said Edith Tutsch-Bauer "We tried desperately to open the door, but we couldn't" Two mile long tunnel.

Appendix B

FDS Material Input Parameters

B1 FDS Material Input Parameters

The following material input parameters were developed through the genetic algorithm analysis discussed in Section 7.4.4.

B1.1 Surfaces

SURF ID	= 'GRP_A'
STRETCH_FACTOR	= 1.000
CELL_SIZE_FACTOR	= 0.500
THICKNESS(01)	= 0.0027
MATL_ID(01,01)	= 'GRP_A_virgin'
MATL_ID(01,02)	= 'GRP_A_char'
MATL_MASS_FRACTION(01,01)	= 1.0000
MATL_MASS_FRACTION(01,02)	= 0.0000
BACKING	='INSULATED'
SHRINK	=.FALSE.
TMP_INNER	= 27.0

SURF ID	= 'GRP_B'
STRETCH_FACTOR	= 1.000
CELL_SIZE_FACTOR	= 0.500
THICKNESS(01)	= 0.0035
MATL_ID(01,01)	= 'GRP_B_virgin'
MATL_ID(01,02)	= 'GRP_B_char'
MATL_MASS_FRACTION(01,01)	= 1.0000
MATL_MASS_FRACTION(01,02)	= 0.0000
BACKING	='INSULATED'
SHRINK	=.FALSE.
TMP_INNER	= 27.0

B1.2 Materials

MATL ID = 'GRP_A_virgin'
CONDUCTIVITY_RAMP = 'GRP_A_RAMP_01'
DENSITY = 1721.00
SPECIFIC_HEAT_RAMP = 'GRP_A_RAMP_02'
EMISSIVITY = 0.864
ABSORPTION_COEFFICIENT = 0.1000E+07
RESIDUE(01) = 'GRP_A_char'
A(01) = 0.7442E+09
E(01) = 0.1229E+06
N_S(01) = 1.21
HEAT_OF_REACTION(01) = 1636.08
NU_FUEL(01) = 0.400
NU_RESIDUE(01) = 0.600
NU_WATER(01) = 0.000
N_REACTIONS = 1

MATL ID = 'GRP_A_char'
CONDUCTIVITY_RAMP = 'GRP_A_RAMP_03'
DENSITY = 1032.60
SPECIFIC_HEAT_RAMP = 'GRP_A_RAMP_04'
EMISSIVITY = 0.927
ABSORPTION_COEFFICIENT = 0.1000E+07
N_REACTIONS = 0

MATL ID = 'GRP_B_virgin'
CONDUCTIVITY_RAMP = 'GRP_B_RAMP_01'
DENSITY = 1312.57
SPECIFIC_HEAT_RAMP = 'GRP_B_RAMP_02'
EMISSIVITY = 0.867
ABSORPTION_COEFFICIENT = 0.1000E+07
RESIDUE(01) = 'GRP_B_char'
A(01) = 0.2284E+10
E(01) = 0.1344E+06
N_S(01) = 1.50
HEAT_OF_REACTION(01) = 682.84
NU_FUEL(01) = 0.544
NU_RESIDUE(01) = 0.456
NU_WATER(01) = 0.000
N_REACTIONS = 1

MATL ID = 'GRP_B_char'
CONDUCTIVITY_RAMP = 'GRP_B_RAMP_03'
DENSITY = 598.91
SPECIFIC_HEAT_RAMP = 'GRP_B_RAMP_04'
EMISSIVITY = 0.924
ABSORPTION_COEFFICIENT = 0.1000E+07
N_REACTIONS = 0

B1.3 Ramps

RAMP ID = 'GRP_A_RAMP_01', T= 27.0, F = 0.2551 /
RAMP ID = 'GRP_A_RAMP_01', T= 127.0, F = 0.3190 /
RAMP ID = 'GRP_A_RAMP_01', T= 227.0, F = 0.3794 /
RAMP ID = 'GRP_A_RAMP_01', T= 327.0, F = 0.4372 /
RAMP ID = 'GRP_A_RAMP_01', T= 427.0, F = 0.4929 /
RAMP ID = 'GRP_A_RAMP_01', T= 527.0, F = 0.5468 /
RAMP ID = 'GRP_A_RAMP_01', T= 627.0, F = 0.5992 /
RAMP ID = 'GRP_A_RAMP_01', T= 727.0, F = 0.6504 /
RAMP ID = 'GRP_A_RAMP_01', T= 827.0, F = 0.7004 /
RAMP ID = 'GRP_A_RAMP_01', T= 927.0, F = 0.7494 /

RAMP ID = 'GRP_A_RAMP_02', T= 27.0, F = 1.4095 /
RAMP ID = 'GRP_A_RAMP_02', T= 127.0, F = 1.8486 /
RAMP ID = 'GRP_A_RAMP_02', T= 227.0, F = 2.2814 /
RAMP ID = 'GRP_A_RAMP_02', T= 327.0, F = 2.7092 /
RAMP ID = 'GRP_A_RAMP_02', T= 427.0, F = 3.1329 /
RAMP ID = 'GRP_A_RAMP_02', T= 527.0, F = 3.5532 /
RAMP ID = 'GRP_A_RAMP_02', T= 627.0, F = 3.9704 /
RAMP ID = 'GRP_A_RAMP_02', T= 727.0, F = 4.3851 /
RAMP ID = 'GRP_A_RAMP_02', T= 827.0, F = 4.7973 /
RAMP ID = 'GRP_A_RAMP_02', T= 927.0, F = 5.2074 /

RAMP ID = 'GRP_A_RAMP_03', T= 27.0, F = 0.1326 /
RAMP ID = 'GRP_A_RAMP_03', T= 127.0, F = 0.1626 /
RAMP ID = 'GRP_A_RAMP_03', T= 227.0, F = 0.1905 /
RAMP ID = 'GRP_A_RAMP_03', T= 327.0, F = 0.2168 /
RAMP ID = 'GRP_A_RAMP_03', T= 427.0, F = 0.2419 /
RAMP ID = 'GRP_A_RAMP_03', T= 527.0, F = 0.2660 /
RAMP ID = 'GRP_A_RAMP_03', T= 627.0, F = 0.2892 /
RAMP ID = 'GRP_A_RAMP_03', T= 727.0, F = 0.3116 /
RAMP ID = 'GRP_A_RAMP_03', T= 827.0, F = 0.3334 /
RAMP ID = 'GRP_A_RAMP_03', T= 927.0, F = 0.3547 /

RAMP ID = 'GRP_A_RAMP_04', T= 27.0, F = 1.4671 /
RAMP ID = 'GRP_A_RAMP_04', T= 127.0, F = 1.9185 /
RAMP ID = 'GRP_A_RAMP_04', T= 227.0, F = 2.3622 /
RAMP ID = 'GRP_A_RAMP_04', T= 327.0, F = 2.7999 /
RAMP ID = 'GRP_A_RAMP_04', T= 427.0, F = 3.2327 /
RAMP ID = 'GRP_A_RAMP_04', T= 527.0, F = 3.6614 /
RAMP ID = 'GRP_A_RAMP_04', T= 627.0, F = 4.0864 /
RAMP ID = 'GRP_A_RAMP_04', T= 727.0, F = 4.5082 /
RAMP ID = 'GRP_A_RAMP_04', T= 827.0, F = 4.9272 /
RAMP ID = 'GRP_A_RAMP_04', T= 927.0, F = 5.3436 /

```
RAMP ID = 'GRP_B_RAMP_01', T=   27.0, F =  0.1697 /
RAMP ID = 'GRP_B_RAMP_01', T=  127.0, F =  0.1880 /
RAMP ID = 'GRP_B_RAMP_01', T=  227.0, F =  0.2036 /
RAMP ID = 'GRP_B_RAMP_01', T=  327.0, F =  0.2172 /
RAMP ID = 'GRP_B_RAMP_01', T=  427.0, F =  0.2295 /
RAMP ID = 'GRP_B_RAMP_01', T=  527.0, F =  0.2406 /
RAMP ID = 'GRP_B_RAMP_01', T=  627.0, F =  0.2509 /
RAMP ID = 'GRP_B_RAMP_01', T=  727.0, F =  0.2605 /
RAMP ID = 'GRP_B_RAMP_01', T=  827.0, F =  0.2695 /
RAMP ID = 'GRP_B_RAMP_01', T=  927.0, F =  0.2780 /

RAMP ID = 'GRP_B_RAMP_02', T=   27.0, F =  1.5710 /
RAMP ID = 'GRP_B_RAMP_02', T=  127.0, F =  1.7824 /
RAMP ID = 'GRP_B_RAMP_02', T=  227.0, F =  1.9658 /
RAMP ID = 'GRP_B_RAMP_02', T=  327.0, F =  2.1295 /
RAMP ID = 'GRP_B_RAMP_02', T=  427.0, F =  2.2786 /
RAMP ID = 'GRP_B_RAMP_02', T=  527.0, F =  2.4161 /
RAMP ID = 'GRP_B_RAMP_02', T=  627.0, F =  2.5442 /
RAMP ID = 'GRP_B_RAMP_02', T=  727.0, F =  2.6647 /
RAMP ID = 'GRP_B_RAMP_02', T=  827.0, F =  2.7785 /
RAMP ID = 'GRP_B_RAMP_02', T=  927.0, F =  2.8866 /

RAMP ID = 'GRP_B_RAMP_03', T=   27.0, F =  0.1097 /
RAMP ID = 'GRP_B_RAMP_03', T=  127.0, F =  0.1215 /
RAMP ID = 'GRP_B_RAMP_03', T=  227.0, F =  0.1316 /
RAMP ID = 'GRP_B_RAMP_03', T=  327.0, F =  0.1405 /
RAMP ID = 'GRP_B_RAMP_03', T=  427.0, F =  0.1484 /
RAMP ID = 'GRP_B_RAMP_03', T=  527.0, F =  0.1556 /
RAMP ID = 'GRP_B_RAMP_03', T=  627.0, F =  0.1623 /
RAMP ID = 'GRP_B_RAMP_03', T=  727.0, F =  0.1685 /
RAMP ID = 'GRP_B_RAMP_03', T=  827.0, F =  0.1744 /
RAMP ID = 'GRP_B_RAMP_03', T=  927.0, F =  0.1799 /

RAMP ID = 'GRP_B_RAMP_04', T=   27.0, F =  1.5935 /
RAMP ID = 'GRP_B_RAMP_04', T=  127.0, F =  1.7960 /
RAMP ID = 'GRP_B_RAMP_04', T=  227.0, F =  1.9706 /
RAMP ID = 'GRP_B_RAMP_04', T=  327.0, F =  2.1257 /
RAMP ID = 'GRP_B_RAMP_04', T=  427.0, F =  2.2664 /
RAMP ID = 'GRP_B_RAMP_04', T=  527.0, F =  2.3958 /
RAMP ID = 'GRP_B_RAMP_04', T=  627.0, F =  2.5161 /
RAMP ID = 'GRP_B_RAMP_04', T=  727.0, F =  2.6287 /
RAMP ID = 'GRP_B_RAMP_04', T=  827.0, F =  2.7350 /
RAMP ID = 'GRP_B_RAMP_04', T=  927.0, F =  2.8358 /
```